Materials Horizons

ROYAL SOCIETY OF CHEMISTRY

REVIEW

View Article Online
View Journal

Check for updates

Cite this: DOI: 10.1039/d5mh00279f

Innovative biosensing smart masks: unveiling the future of respiratory monitoring

Jiahui Liang, Conghui Liu * and Tailin Xu

Received 17th February 2025,
Accepted 30th April 2025

DOI: 10.1039/d5mh00279f

rsc.li/materials-horizons

Real-time monitoring of respiratory health is increasingly critical, particularly in addressing global health challenges such as Corona Virus Disease 2019 (COVID-19). Smart masks equipped with biosensing mechanisms revolutionize respiratory health monitoring by enabling real-time detection of respiratory parameters and biomarkers. In recent years, significant advancements have been achieved in the development of smart masks based on different sensor types with high sensitivity and accuracy, flexible functionality, and portability, providing new approaches for remote and real-time monitoring of respiratory parameters and biomarkers. In this review, we aim to provide a comprehensive overview of the current state of development and future potential of biosensing smart masks in various domains. This review outlines a systematic categorization of smart masks according to diverse sensing principles, classifying them into six categories: electrochemical sensors, optical sensors, piezoelectric sensors, and others. This review discusses the basic sensing principles and mechanisms of smart masks and describes the existing research developments of their different biosensors. Additionally, it explores the innovative applications of smart masks in health monitoring, protective functions, and expanding application scenarios. This review also identifies the current challenges faced by smart masks, including issues with sensor accuracy, environmental interference, and the need for better integration of multifunctional features. Proposed solutions to these challenges are discussed, along with the anticipated role of smart masks in early disease detection, personalized medicine, and environmental protection.

Wider impact

A significant development in this research area is the integration of multiple biosensing technologies into smart masks, the classification of smart masks according to the detection principle, and the real-time monitoring of respiratory parameters and biomarkers. The application of these technologies expands the function of masks from pure protection to health monitoring. This field is of great significance for two principal reasons. Firstly, within the domain of health, it can detect diseases such as lung cancer and cardiovascular at an early stage, thereby facilitating early intervention for patients. Secondly, in the context of environmental monitoring, it can detect harmful gases and microorganisms, thus ensuring the safety of the living environment. This is of far-reaching significance for both personal health and public health. In the future, the field will evolve towards enhancing the performance of sensors and the integration of masks to ensure more accurate and comprehensive monitoring. Furthermore, there will be an emphasis on improving wearing comfort and safety. This review provides research and development ideas in materials science to assist in the development of highly sensitive, stable and biocompatible sensing materials.

1. Introduction

The global Corona Virus Disease 2019 (COVID-19) pandemic has significantly increased the reliance on masks as an essential tool for reducing viral transmission.[1,2] Traditional masks primarily serve protective roles by filtering harmful particles such as viruses, bacteria, and dust,[3] while also enabling cleaner air intake[4] and reducing the spread of droplets during exhalation.[5] During the COVID-19 pandemic, masks significantly inhibited the spread of the virus and greatly protected lives.[6–8] However, the focus on protection alone has highlighted a gap in personal health monitoring, prompting the emergence of smart masks. Equipped with advanced biosensors, smart masks extend beyond basic protection, offering real-time, non-invasive monitoring of respiratory health. With increasing focus on personal health and safety, smart masks integrated with advanced biosensors present a promising solution for real-time and non-invasive monitoring of respiratory parameters[9] and biomarker detection in exhaled breath,[10–13] offering real-time, non-invasive monitoring of respiratory health. These smart masks are not only designed for

College of Chemistry and Environmental Engineering, Institute for Advanced Study, Shenzhen University, Shenzhen, Guangdong 518060, P. R. China.
E-mail: conghuiliu@szu.edu.cn

filtering contaminants but also incorporate functionalities such as self-powering,[14,15] eco-friendliness,[16,17] antibacterial,[18–20] and antiviral[21–23] properties, which enhance their potential applications in early disease warning,[9,13] health monitoring,[24–26] environmental tracking,[5] and more.

Despite the promise of smart masks, existing technologies for detecting respiratory biomarkers have been limited by the need for specialized, bulky equipment typically found in clinical settings. These traditional methods require hospital visits, restricting their frequency and accessibility. This limitation underscores the pressing need for portable, intelligent testing devices that can offer continuous, real-time health monitoring. Recent advancements in smart mask technology have addressed these challenges by integrating biosensing technologies capable of detecting various biomarkers directly from exhaled breath, offering a non-invasive approach for tracking respiratory health. These innovations enable the early detection of diseases such as COPD,[27–30] cardiovascular disease,[31,32] and asthma,[33–35] making smart masks a powerful tool for health management.

As with previous works, these reviews have summarized the applications on materials,[36] storage devices,[37] and health monitoring of wearable devices.[38] The current paper focuses on sensing principles and innovations of smart masks. We aim to provide an in-depth exploration of the biosensing mechanisms behind these devices, emphasizing their role in real-time respiratory monitoring. We will discuss the main sensing technologies, such as electrochemical, optical, piezoelectric, and bioaffinity sensors, and examine their respective strengths and limitations. In this review, we also highlight recent advances in smart mask functionality, including the integration of self-powered systems and dosimetry capabilities. The review will also explore the expanding applications of smart masks, from early disease detection to environmental monitoring, and discuss the challenges faced in scaling these technologies for widespread use. Finally, we will consider the prospects of smart masks as wearable health devices, addressing both the technological hurdles that need to be overcome and the wider societal impact that these innovations may have on healthcare and environmental safety.

2. Health monitoring process

This section focuses on the health monitoring process in smart masks. Fig. 1 visually captures the mechanisms behind smart masks—from biomarker detection to sensing technologies and finally, the signal output. These devices transform biological signals into actionable health data that can be monitored and analyzed through digital platforms, providing users with continuous, real-time insights into their respiratory health. The integration of these sensing methods offers a less invasive alternative to traditional diagnostic tools, enabling early disease detection and personalized healthcare monitoring. By explaining these mechanisms in the text, the functionality of smart masks becomes clearer, showcasing their potential in health monitoring, protective functions, and broader applications for personalized health management and environmental monitoring.

2.1 Respiratory biomarkers

The human body releases a variety of biomarkers during respiration, including volatile organic compounds (VOCs),[39]

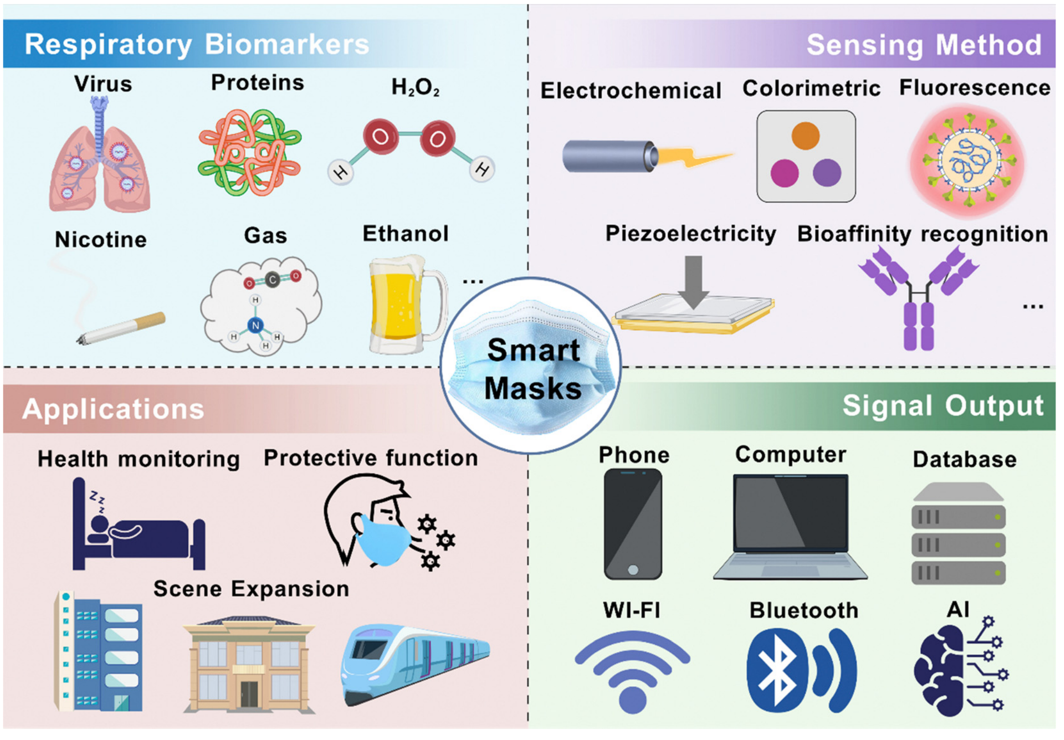

Fig. 1 Overview of the health monitoring process in smart masks. This schematic was created with BioGDP.

semi-volatile organic compounds (SVOCs),[40] various types of gases (oxygen,[41] carbon dioxide,[42] ammonia,[43] *etc.*), exhaled breath condensate (EBC),[44] proteins,[45] and viruses,[46] among others.[47] With growing health awareness, detecting biomarkers *via* smart masks is emerging as one of the most direct and effective diagnostic methods. Illnesses can alter physiological indicators, leading to changes in the composition of respiratory gas. The detection of these components in exhaled breath is important for real-time monitoring of human health, as it provides a non-invasive method of assessing the physiological state of the body. These biomarkers change in concentration as a response to physiological changes or diseases, and their detection offers valuable insights into health status, making them critical for health monitoring (*e.g.*, diagnosing lung diseases, kidney dysfunction, or even viral infections). Table 1 summarizes smart masks for biomarker and disease monitoring. Smart masks serve as an alternative, less invasive diagnostic method compared to traditional testing procedures, offering real-time, continuous monitoring. As shown in Table 1, the detection of VOCs and SVOCs is critical for diseases such as lung cancer, with smart masks like polyurethane foam face masks and fabric masks designed to measure these biomarkers at low concentrations. The polyaromatic hydrocarbons and ethanol biomarkers, which are associated with diseases like lung cancer, gastric ulcers, and pancreatitis, are detectable with a variety of smart masks, including polyurethane-based face masks and room-temperature ethanol sensors. Table 1 also introduces other advanced monitoring systems, such as the exhaling-oxygen-sensing mask, which plays a crucial role in diseases like COPD, asthma, and other pulmonary conditions by tracking oxygen levels, a vital indicator of lung function. Moreover, bioelectronic masks are mentioned, which are used for detecting surface proteins of viruses, providing a means for monitoring viral infections like respiratory diseases, and enabling real-time detection of viral markers. In terms of disease diagnosis, the smart mask provides a less invasive alternative to traditional diagnostic methods. Advancing research on biomarkers and their detection methods could enable more precise early disease diagnosis and effective personalized treatments.

2.2 Sensing method

Miniaturizing biosensors integrated into masks is crucial for non-invasive, real-time, on-site detection. These sensors are typically placed under the nose or embedded within the mask. To ensure accurate and rapid biomarker detection, these sensors require high sensitivity, selectivity, resistance to environmental interference, long-term durability, fast response times, and low detection limits. Biosensors in most smart masks are primarily based on electrochemical, optical, piezoelectric, bioaffinity recognition, temperature-sensing, and humidity-sensing mechanisms[57] (Fig. 2).

Electrochemical sensors detect potential differences between electrodes, enabling them to classify into potentiometric sensors, which measure changes in electrode potential due to redox reactions, and amperometric (current) sensors, which monitor current variations during redox reactions at a fixed potential. These sensors offer high sensitivity, real-time monitoring, and adaptability for miniaturization, making them suitable for wearable designs.[58–60] However, their electrodes are fragile, and external factors can easily affect the signal stability. Optical sensors, including fluorescence detection, are commonly employed for virus detection, where biomarkers are quantified by measuring fluorescence intensity at a specific excitation wavelength.[61,62] Although affordable and simple to use, optical sensors are susceptible to background fluorescence interference and quenching effects. Additionally, colorimetry sensors utilize biochemical or hydrolytic reactions between gas molecules and

Table 1 Overview of smart masks for biomarker and disease monitoring

Biomarkers	Related diseases	Type of mask	LOD	Functionality	limitation	Ref.
VOCs and SOVs	Lung cancer	Polyurethane foam face masks	—	Dosimeter	Complex analysis process	48
Polycyclic aromatic hydrocarbons	Lung cancer	Fabric masks	0.04 ng m^{-3} 0.02–0.04 ng m^{-3} 0.03–0.05 ng m^{-3} 0.03–0.06 ng m^{-3} 0.05 ng m^{-3}	Dosimeter	Affected by the environment	49
ETS	Lung cancer	Polyurethane-based face mask	0.20 mg m^{-3} 5.2 mg m^{-3}	Sampling medium	Single-substance detection	50
Ethanol	Cirrhosis, gastric ulcer, pancreatitis	Room-temperature ethanol sensor	10 ppb	DUI monitoring	Cross-sensitivity	51
$C_6H_{12}O_6$	Diabetes	Mask-based printing electrodes	0.1 μM	Blood glucose testing	Interference with detection accuracy	52
NH_3	Chronic kidney disease	Respiration sensor	1 ppb	Biomarker monitoring	Biomarker specificity issues	53
NH_3; volatile sulfur compound (VSC)	Kidney disease	Flexible waste mask sensors	100 ppb	Human and environmental ammonia monitoring	Cross-sensitivity	54
O_2	Chronic obstructive pulmonary disease (COPD), asthma and other lung diseases	Exhaling-oxygen-sensing mask	—	Assessment of pulmonary oxygenation capacity	Individual differences affect	55
Surface proteins of viruses	Viral infections, respiratory infections	Bioelectronic masks	0.1 fg mL^{-1}	Multi-target simultaneous detection	Insufficient clinical validation	56

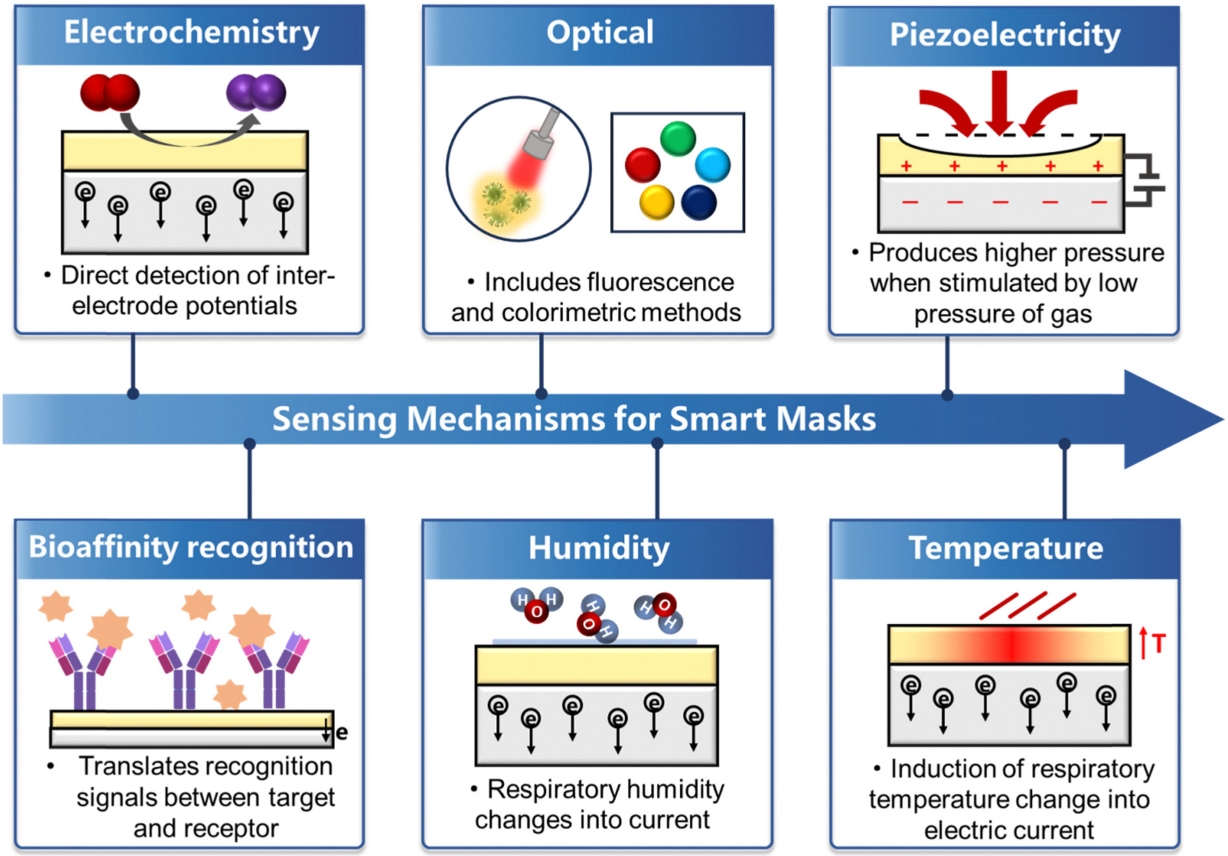

Fig. 2 Sensing mechanisms for sensor masks including electrochemical sensing, optical (fluorescence, colorimetric, *etc.*), piezoelectric sensing, bioaffinity recognition sensing, and temperature sensing.

color-changing reagents to produce a visual signal.[63–65] Similar to fluorescence detection, colorimetry is accessible and easy to use but suffers from limitations in sensitivity and precision, particularly for multi-component quantitative analysis.

Piezoelectric sensors detect airflow pressure during breathing, which deforms the material and displaces charge centers, generating an electrical charge on the surface.[66–69] These sensors are reliable for detecting respiratory signals with high sensitivity and reproducibility, though their detection limit tends to be higher. Bioaffinity recognition sensors rely on specific interactions between target biomarkers and receptors to generate measurable signals, enabling the detection of specific bioreceptors.[70] However, these sensors are limited by the number of available receptors and can have reduced stability over time. Humidity sensors operate by detecting changes in mask humidity during breathing, with alteration in the material's potential caused by the absorption or release of water molecules.[71–73] Temperature sensors function similarly by measuring changes in air temperature, which affect the material's electrical potential.[74–76] Both humidity and temperature sensors are simple and cost-effective, but are highly influenced by external environmental factors. These diverse sensing mechanisms enable smart masks to effectively monitor a wide range of biomarkers and environmental conditions, paving the way for improved health monitoring and disease detection.

2.3 Signal output

The capacity of smart masks to capture a rich and diverse set of detection signal data during real-world use is made possible by the integration of advanced biomarker detection technology and various sensing methods, as illustrated in Fig. 1. These technologies enable the identification of respiratory biomarkers, such as viruses, proteins, and gases, as well as their concentrations in real time. Electrochemical sensors, for instance, detect small variations in current or potential resulting from chemical reactions between biomarkers and electrodes, providing reliable data for the quantification of biomarkers. Similarly, fluorescence-based sensors measure the intensity of emitted light, reflecting changes in the optical properties of biomarkers upon reaction with specific reagents. Despite the promising capabilities of these sensors, signal acquisition can be challenging due to environmental interference, which affect the accuracy of readings. To address this, the raw signals are subjected to processing steps, such as noise reduction and signal amplification, ensuring the data's reliability. Once processed, the data are compared with established digital models to calculate biomarker concentrations of biomarkers in breath samples. These data are then transmitted to external devices, such as a computer or smartphone, using wireless technologies like Wi-Fi or Bluetooth. The use of big data analytics, coupled with the Internet of Things (IoT),[11,77–80] facilitates the real-time health monitoring and the early detection of disease.[81,82] By analyzing these biomarker levels, smart masks can offer insights into potential health risks, helping users make informed decisions about their well-being. Mobile applications enable users to access real-time test results, while healthcare professionals can perform more detailed evaluations using advanced data analysis tools available on computers. This integration of big data, IoT, and advanced sensing technologies is propelling healthcare toward more personalized, precise, and intelligent solutions.

3. Application of smart masks based on different sensing modalities

3.1 Electrochemical sensors

With high sensitivity and real-time monitoring capability, electrochemical sensors have become the core technology for detecting trace metabolites in exhaled breath. However, challenges such as humidity interference, low analyte concentration, and the need for non-invasive, continuous operation limit their broader clinical translation. Recent research has addressed these issues from multiple angles, including device design, sensing mechanisms, and materials innovation.

To achieve efficient sample collection and automation, Heng *et al.* developed the EBCare mask, an integrated system for capturing and analyzing EBC (Fig. 3(a)).[83] The device incorporates hydrogel-based evaporative cooling, metamaterial radiative cooling, high thermal conductivity materials, and a capillary force gradient to automate EBC condensation, transfer, and detection, demonstrating feasibility for real-time, user-friendly metabolite tracking. Focusing on H_2O_2 detection as a representative volatile marker, Maier *et al.* introduced a disposable, paper-based electrochemical sensor using Prussian blue (PB) as the redox mediator.[84] H_2O_2 oxidizes the PB in the electrolytic cell to generate a cathodic current, which is then recorded *via* differential electrochemical measurements. However, the identification of a stable, effective electrolyte (humectant) remains an unresolved issue in maintaining sensor performance. Building on PB-based strategies, Cao *et al.* developed a polyaniline/PB nanolayer (nano-PANI/PB)-coated electrode (Fig. 3(b)). This electrode efficiently collected gas condensate from the mouthpiece and transferred it to an SPCE plate for H_2O_2 detection. This innovation represents a notable advancement in portable detection technology.[85] Beyond conventional sensing, Jeerapan *et al.* designed a self-powered bioelectronic sensor using a glucose biofuel cell framework.[52] By immobilizing glucose oxidase and tetrathiophene at the anode, the system generates electrons from glucose oxidation, enabling continuous glucose detection with a sensitivity limit of 0.22 mM. This approach eliminates the need for external power, offering advantages for long-term wearable use. In terms of material innovation, $Ti_3C_2T_x$ MXenes have gained significant attention for their excellent conductivity and surface tunability. Li *et al.* developed $Ti_3C_2T_x$–M2-based gas sensors with reduced humidity interference and enhanced ethanol sensing performance (Fig. 3(c)).[86] The sensing mechanism involves a "sheet-seeing" effect, where gas intercalation increases resistance. A 71% reduction in water vapor response and a five-fold increase in ethanol sensitivity were achieved by exploiting weak H_2O–$Ti_3C_2T_x$–M2 interactions. Extending this strategy, the same group designed a $Ti_3C_2T_x$ MXene-based mask capable of

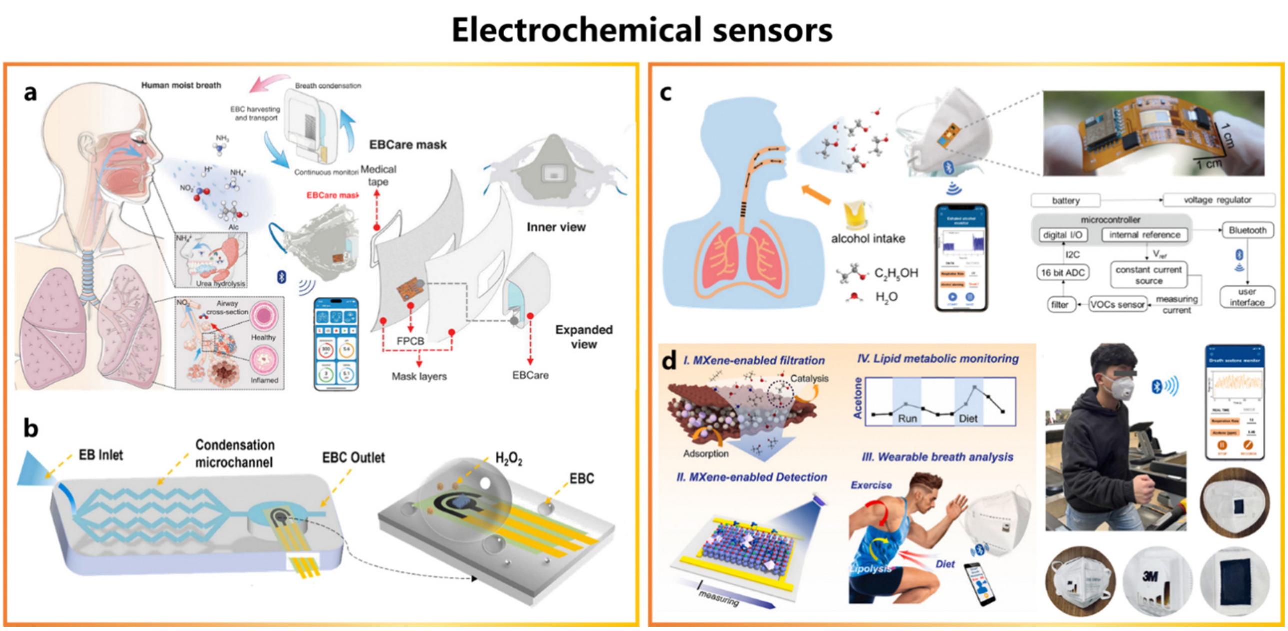

Fig. 3 Application of electrochemical sensors in masks. (a) A smart EBCare mask for efficient harvesting and continuous analysis of exhaled breath condensate.[83] Copyright 2024 Science. (b) Portable hydrogen peroxide in exhaled breath detection device.[85] Copyright 2023 Sensors and Actuators B: Chemical. (c) The schematic illustration of wearable monitoring of exhaled breath ethanol after alcohol intake. Reproduced with permission from ref. 86. Copyright 2021 Advanced Materials Technologies. (d) Photograph of a human body wearing a mask during exercise and schematic diagram of the acetone sensing principle. Reproduced with permission from ref. 87. Copyright 2023 Biosensors and Bioelectronics.

detecting breath acetone (BrAc) at concentrations as low as 0.31 ppm (Fig. 3(d)).[87] BrAc adsorption increases the distance between MXene nanosheets, leading to higher resistance.

For practical alcohol monitoring, Wu's group fabricated a composite sensor using PP/$Ti_3C_2T_x$/PPy, where the amino groups in PPy capture ethanol molecules, and $Ti_3C_2T_x$ expand the connecting channels to enhance the adsorption.[51] The material was implemented in a breathalyzer for DUI monitoring, offering stable and reproducible ethanol sensing.

These advances highlight the adaptability of electrochemical sensors for breath analysis. However, consistent challenges, such as miniaturization with multianalyte capability, interference suppression, and long-term calibration, still require systematic investigation.

3.2 Optical sensors

Optical sensors can be categorized into two primary methods: fluorescence emission and absorbance monitoring (colorimetric methods). These sensors are suitable for rapid screening with the advantages of low cost and visualization. However, key challenges remain in terms of environmental interference, sensitivity to humidity, and signal stability in wearable and non-invasive formats. Recent innovations in mask-based optical platforms have sought to address these limitations through intelligent material integration and signal amplification techniques.

Fluorescence sensors detect biomarkers by measuring light absorption at specific wavelengths, often utilizing energy transfer or quenching mechanisms. For instance, Zhang *et al.* developed a Janus wettable mask incorporating a proportional fluorescent probe for H_2S detection (Fig. 4(a)).[88] The system utilizes red-emitting silver clusters (AgNCs) and blue-emitting carbon dots (CDs), achieving a visible fluorescence shift from red to blue upon H_2S exposure. This ratiometric approach enabled a detection limit as low as 0.8 ppb, offering high sensitivity in a visually intuitive format. Inspired by the remarkable water-collecting ability of nanofabricated desert beetles, Chen *et al.* developed a surface-wettability-based strategy to enhance Raman scattering signals on mask surfaces (Fig. 4(b)).[89] By directing respiratory droplets toward SERS-active regions, the platform achieved nitrite detection with a detection limit as low as 10^{-16} M, demonstrating a solution for trace analyte enrichment in EBC. Escobedo *et al.* took a different approach by embedding a CO_2-responsive fluorescent sensor into an FFP2 mask, enabling continuous respiration monitoring.[90] The sensor, composed of inorganic phosphors and acid–base indicators, was activated by an NFC-enabled mobile phone, facilitating real-time read-outs of respiratory CO_2 acidity without external instrumentation.

Colorimetric methods involve biochemical or hydrolytic reactions between biomarkers and specific dyes, providing a clear and visual readout. These systems are particularly attractive

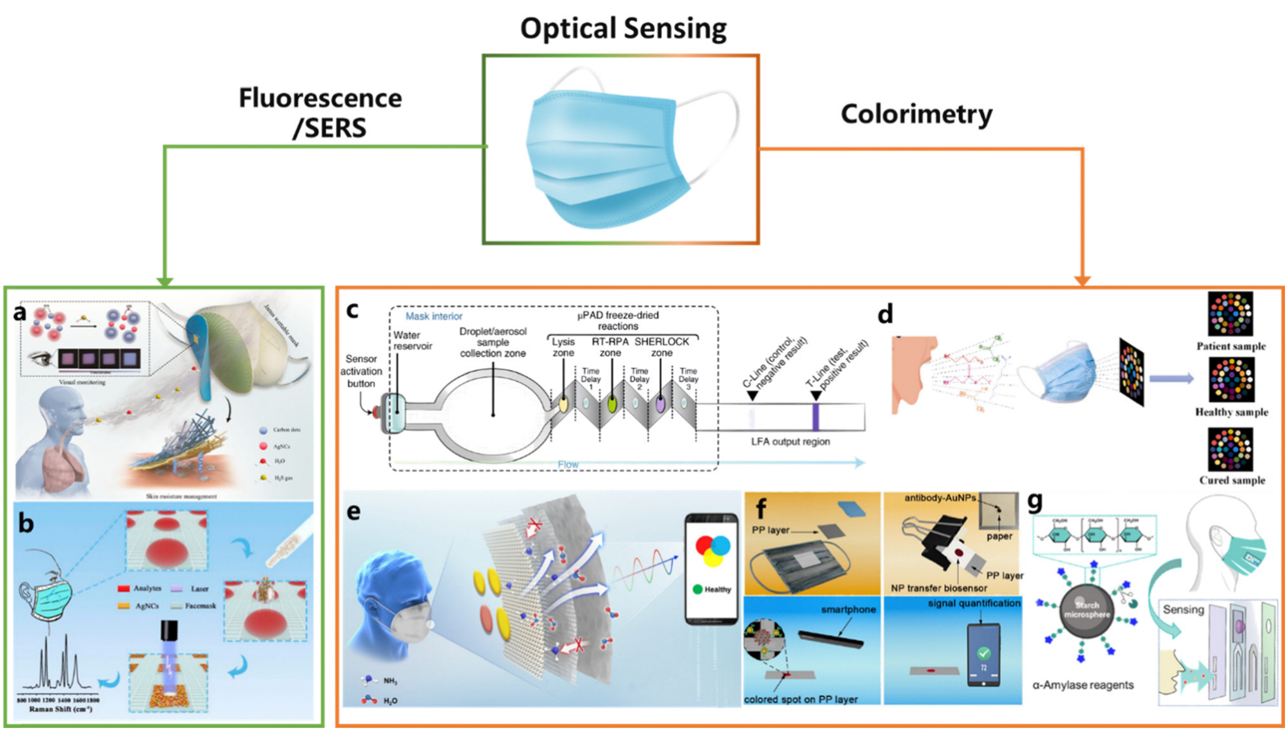

Fig. 4 Application of optical sensors in masks. (a) Schematic illustration of a Janus wettable mask with an integrated ratiometric fluorescent probe.[88] Copyright 2024 ACS Sensors. (b) Schematic illustration for *in situ* collecting and analyzing nitrite with SERS on a Facemask@AgNCs@4-ATP. Reproduced with permission from ref. 89. Copyright 2024 ACS Sensors. (c) Schematic of a face-mask-integrated SARS-CoV-2 wearable diagnostic.[91] Copyright 2021 Nature Biotechnology. (d) A colorimetric breath sensor was developed for the detection of COVID-19.[92] Copyright 2022 Sensors and Actuators B: Chemical. (e) A wearable Janus colorimetric mask for ammonia sensing.[93] Copyright 2023 Analytical Chemistry. (f) Nanoparticle biosensors detecting SARS-CoV-2 antigens trapped in surgical face masks. Reproduced with permission from ref. 94. Copyright 2021 Sensors and Actuators B: Chemical. (g) Smart mask combining face coverings and sensing strip.[95] Copyright 2021 Analytical Chemistry.

for low-resource settings due to their simplicity and compatibility with smartphone-based analysis. Nguyen's group developed a lyophilized CRISPR sensor embedded in a mask for SARS-CoV-2 detection (Fig. 4(c)).[91] The mask is designed to absorb a sample of the virus carried in the breath onto a microfluidic paper-based analytical device μPAD, which can be lysed and analyzed for viral and nucleic acid components. The resulting colorimetric signal provides a rapid, instrument-free diagnostic output. Bordbar *et al.* proposed an optical sniffing device affixed to the inside of the mask to differentiate between patients, healthy individuals, and cured individuals based on the VOC-triggered color change (Fig. 4(d)).[92] The observed color variation correlated linearly with viral load, enabling estimation of disease severity in real time. Wang *et al.* developed a Janus colorimetric face mask (JCFM), which possesses four pH indicators to quantify ammonia concentrations ranging from 1 to 10 ppm (Fig. 4(e)).[93] The four indicators (bromophenol red, bromophenol blue, bromocresol green, and methyl red) all contain hydroxyl groups that cross-react with ammonia to display different colors. Combined with the Janus design, this system achieves 96% monitoring accuracy. A rapid virus detection strategy was proposed by Vaquer's group, who developed a biosensor equipped with a nanoparticle reservoir embedded in the mask interlayer (Fig. 4(f)).[94] Upon contact with the virus particles, antigen–antibody interactions facilitate sample transfer to paper, where a mobile phone captures and quantifies the resulting colorimetric change within 10 minutes. This method significantly improves detection efficiency and simplifies the detection process. Beyond pathogen detection, Jin *et al.* used the colorimetric approach to quantify α-amylase in respiratory droplets (Fig. 4(g)).[95] α-Amylase releases a blue dye that binds to starch *via* α-1,4-glucosidic bonds, enabling the determination of the concentration and distribution of aerosol droplets ejected from the human body.

3.3 Piezoelectric sensors

When an individual breathes through a mask, the airflow mechanically deforms (compresses or stretches) the internal material of the sensor in a particular direction, inducing an internal polarization and generating an electrical charge on the surface. Once the external force is removed, the sensor returns to its original uncharged state, a phenomenon known as the "piezoelectric effect". Piezoelectric sensors operate on this principle and are particularly suitable for monitoring respiratory parameters due to their ability to respond to slight mechanical changes without requiring an external power source. Moreover, these sensors have rapid response times, making them more suitable for monitoring the respiratory rate rather than detecting trace gases. In recent years, several studies have explored the use of piezoelectric and triboelectric sensors for respiratory monitoring in smart masks. He *et al.* developed a respiration monitoring triboelectric nanogenerator (RM-TENG) that incorporates nanofiber membranes capable of efficiently filtering particles between 0.3 μm and 5 μm. Additionally, the deformation profile of the two triboelectric layers can be analyzed to monitor breathing (Fig. 5(a)).[96] This system not only integrates particle filtration but also enables real-time respiratory monitoring, offering dual functionality that enhances its applicability in health devices. Vázquez *et al.* proposed an all-fabric TENG (AF-TENG) made from high molecular weight polyethylene (UHMWPE) and cotton fabric. This device is capable of transmitting alerts in critical situations like apnea (Fig. 5(b)).[97] Both of these technologies utilize the principle of triboelectric nanogenerators (TENGs), which are sensitive to small variations in respiratory gases. This sensitivity arises from the triboelectrification induced by inhalation and exhalation, opening up new possibilities for TENGs in smart mask applications.

Additionally, Zhang *et al.* reported a biodegradable, highly breathable, self-powered mask manufactured from polylactic acid (PLA), which records respiratory signals based on the electrostatic induction effect of the PLA electret fabric's charge (Fig. 5(c)).[98] Similarly, Yang's group developed a flexible, paper-based pressure-sensing smart mask by integrating MXene-coated tissue paper (MTP) as an intermediate layer. This innovative smart mask exhibits a low detection limit of 1 Pa and a broad detection range of up to 100 kPa, providing exceptional sensitivity and adaptability for human respiration monitoring (Fig. 5(d)).[99] In the further development of pressure sensor technologies, Zhong *et al.* developed an ultrathin pressure sensor with an Au/parylene/Teflon AF membrane, measuring just 5.5 μm in thickness and weighing around 4.5 mg. This miniature sensor uses a wireless readout circuit, allowing ultra-sensitive detection of weak airflow exchanged during respiration.[103] Gao *et al.* introduced piezoelectric sensors that combine functionalized meltblown fibers and optimized conductive materials, using *in situ* sampling and inverse integration strategies for respiration detection in various scenarios (Fig. 5(e)).[100]

Moreover, Ding's group investigated the potential of superelastic hard carbon aerogels (s-HCAs) for use in respiratory monitoring masks with piezoresistive sensors. The unique honeycomb structure of s-HCAs provides excellent compressibility and superelasticity, making them ideal for sensors sensitive to minor respiratory airflow changes (Fig. 5(f)).[101] Roy *et al.* demonstrated the use of electrospun polyvinylidene difluoride (PVDF)/graphene oxide (GO) nanofibres for the preparation of wearable pressure and pyroelectric respiratory sensors. These nanofibers undergo resistance changes when deformed by airflow, enhancing the piezoelectric effect and achieving ultra-high sensitivity to detect pressures as low as 10 Pa (Fig. 5(g)).[102]

3.4 Bioaffinity recognition sensors

Bioaffinity recognition sensors exploit the highly specific binding interactions between biorecognition elements and target biomarkers, including antigen–antibody binding, enzyme–substrate reactions, receptor–ligand interactions, and nucleic acid hybridization. These interactions trigger measurable changes in the physical or chemical properties of the sensing platform, enabling sensitive and selective detection of target analytes. Despite their inherent specificity, such sensors often face challenges in integrating high performance (*e.g.*, sensitivity, response time) with portability and practical applicability, particularly in non-invasive or minimally invasive formats. Addressing these limitations requires

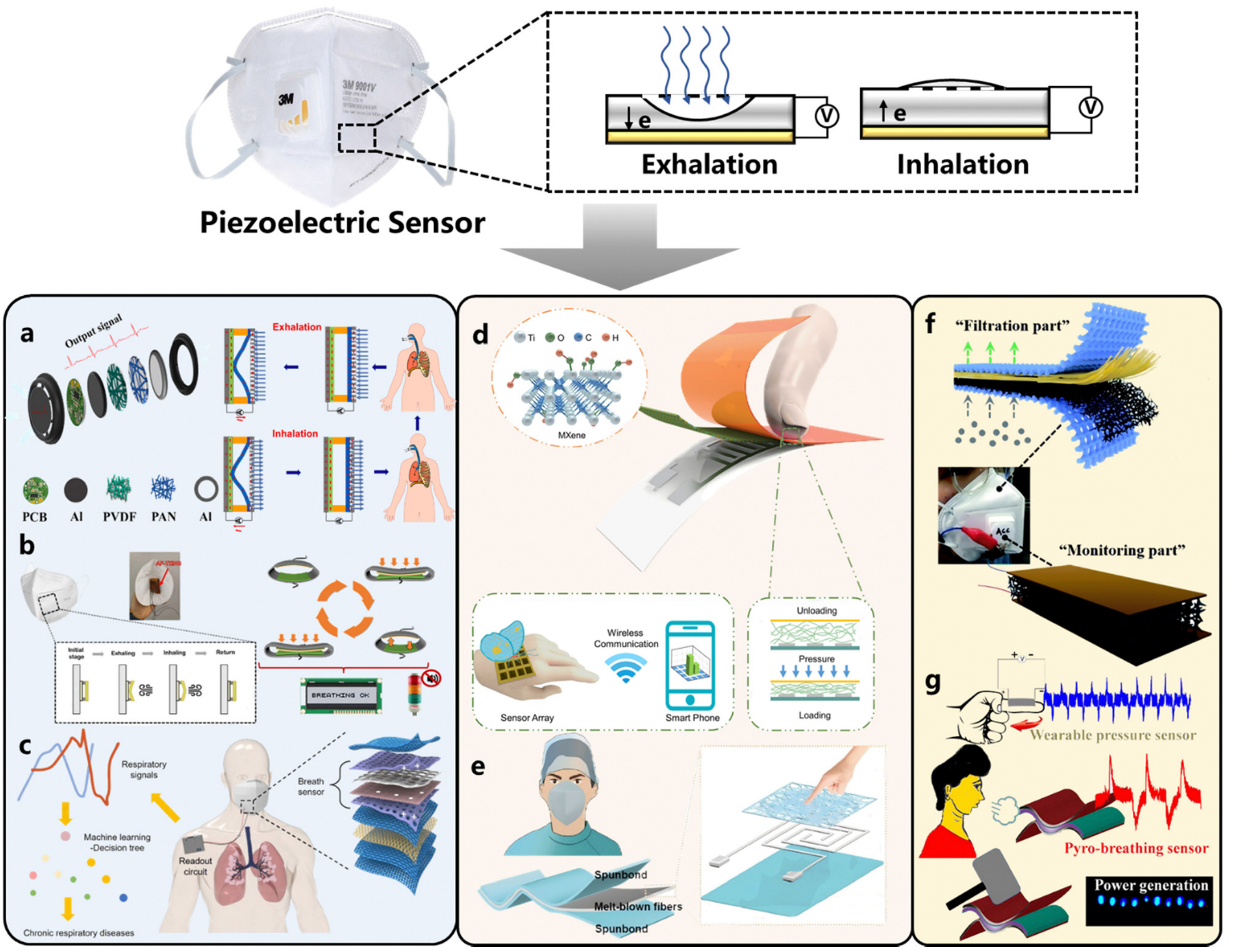

Fig. 5 Application of piezoelectric sensors in masks. (a) Illustration of the working mechanism of the breathing RM-TENG.[96] Copyright 2021 Nano Energy. (b) Working principle and placing of the AF-TENG.[97] Copyright 2023 ACS Sensors. (c) Biodegradable PLA masks for the diagnosis of chronic respiratory diseases.[98] Copyright 2022 ACS Sensors. (d) A novel flexible paper-based pressure sensing platform.[99] Copyright 2021 ACS Applied Materials & Interfaces. (e) Pressure sensing masks based on meltblown fiber pressure sensitive materials.[100] Copyright 2021 IEEE Transactions on Electron Devices. (f) A respiratory monitoring mask with hard carbon aerogels (s-HCAs) as a piezoresistive sensor.[101] Copyright 2021 Journal of Materials Chemistry A. (g) A piezo- and pyro-electric hybrid nanogenerator (NG) device.[102] Copyright 2019 ACS Applied Nano Materials.

innovations in both sensor architecture and biorecognition element integration.

Gutiérrez-Gálvez *et al.* designed a wearable immunosensor by incorporating magnetic beads into N95 masks. Utilizing a sandwich-type immunoassay, this system enables direct capture and detection of SARS-CoV-2 spike proteins from breath samples (as small as 50 μL). Without the need for chemical treatment, the sensor achieved a detection limit of 1 ng mL^{-1}, demonstrating excellent selectivity and practical compatibility (Fig. 6(a)).[70] In another study, Xue *et al.* developed an immunosensor featuring high-density conductive nanowire arrays. The nanowire spacing was optimized to match the viral aerosol dimensions, thereby improving capture efficiency. Specific antibody–antigen interactions were translated into impedance changes for quantitative detection. Impressively, this device detected coronaviruses at concentrations as low as 7 pfu mL^{-1} within just 5 minutes, balancing high sensitivity with rapid response (Fig. 6(b)).[104] These examples demonstrate the combination of advanced material design and biofunctional integration, but further efforts are needed to generalize these systems across broader biosensing applications.

3.5 Humidity sensors

Humidity is a critical physiological parameter that reflects the health of the respiratory mucosa and efficiency of gas exchange in the human body. Humidity sensors can track changes in mask humidity during breathing, converting these changes into electrical signals for data analysis. Kim *et al.* developed a flexible humidity sensor based on carbon nanotubes, which, when paired with a ventilation system, monitors the respiratory rate. The sensor employs a core–shell carbon nanotube structure encapsulating a PAMAM dendrimer G3 (PM), which reacts with water molecules, converting humidity variations into electrical resistance (Fig. 7(a)).[105] Similarly, Chen *et al.* investigated a triple-layered humidity sensor incorporating a nanoforest-based sensing capacitor, a microheater, a reference capacitor, and a thermistor (Fig. 7(b)).

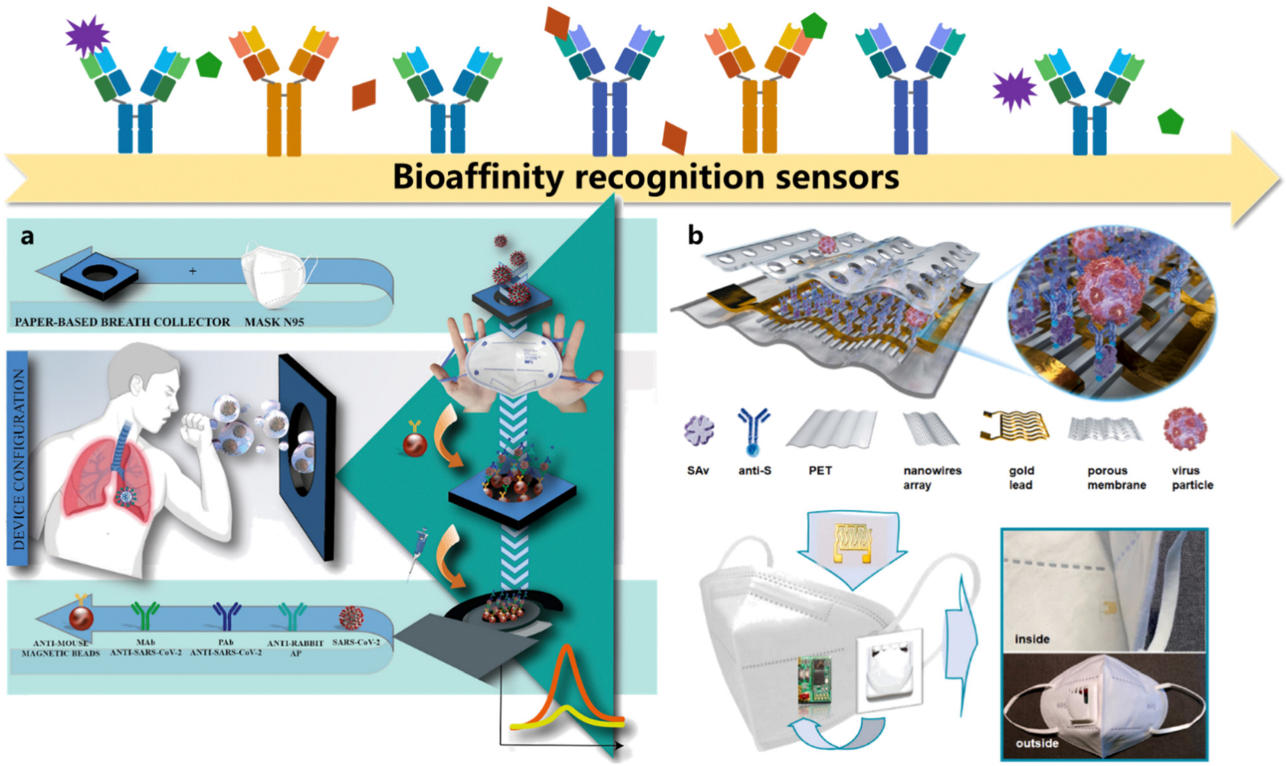

Fig. 6 Application of bioaffinity recognition sensors in masks. (a) Schematic illustration of the developed immunosensor for SARS-CoV-2 Detection in Exhaled Breath.[70] Copyright 2024 ACS Sensors. (b) Smart masks based on high-density conductive nanowire arrays for on-site virus detection.[104] Copyright 2021 Biosensors and Bioelectronics.

The active sites and hydroxyl groups surrounding the nanoforest will be adsorbed by free water molecules through hydrogen bonding. When the first layer of water molecules occupies all the sites, additional water molecules are physically adsorbed, forming multiple layers that increase the capacitance of the sensor as humidity rises.[106]

In another study, He *et al.* developed a humidity sensor using graphene nanochannel-constrained poly(dopamine) (GNCP), a crosslinked polydopamine/graphene (PDA) polymer enriched with hydroxyl (–OH) and amino (–NH_2) groups. This structure facilitates dynamic hydrogen bonding with water molecules, enabling adsorption and desorption (Fig. 7(c)).[107] In a different approach, Güder introduced a paper-based humidity sensor that leverages paper's hygroscopic properties to convert respiration-induced humidity changes into electrical signals (Fig. 7(d)). This low-cost sensor integrates printed graphite electrodes on paper for mask integration. However, this method faces challenges such as high power consumption and electrode cracking when the mask is folded.[108]

Wang *et al.* developed a porous polymer humidity sensor using PVDF/TPU/C, which is capable of generating H_3O^+ ions through the Grotthuss chain reaction, enhancing ionic transport and reducing resistance (Fig. 7(e)).[109] Honda *et al.* designed a flexible humidity-sensing mask for wireless health monitoring during sleep. The mask utilizes $ZnIn_2S_4$ nanosheets as the sensing material, where changes in humidity alter the conductivity of the sensor, providing real-time humidity data (Fig. 7(f)).[110] Similarly, Duan's group developed a multifunctional humidity sensor using printed paper and flexible conductive tape, based on a principle similar to Chen's nanoforest-based sensor. This sensor exhibited a favorable sensing response across a humidity range of 41.1 to 91.5% RH.[111]

These studies highlight the diverse approaches to humidity sensing in smart masks, showcasing innovations in materials and sensor designs that enhance the sensitivity and applicability of these devices for respiratory health monitoring. Through advancements in sensor technologies, including the use of carbon nanotubes, nanoforests, and flexible materials, researchers are continually pushing the boundaries of what is possible in low-cost, efficient, and responsive humidity monitoring systems. These developments pave the way for more integrated, real-time health monitoring solutions, particularly in wearable devices such as smart masks.

3.6 Temperature sensors

Like humidity, temperature is a crucial physiological indicator of human health. Human body temperature fluctuates in response to the respiratory rate, gas exchange efficiency, and external environmental conditions. Temperature sensors are designed to measure both body and environmental temperatures, and in addition to monitoring vital signs, they also serve as an early warning system for environmental changes. Kim *et al.* developed a thermochromic sensor based on aligned controllable electrospinning technology. The sensor membrane

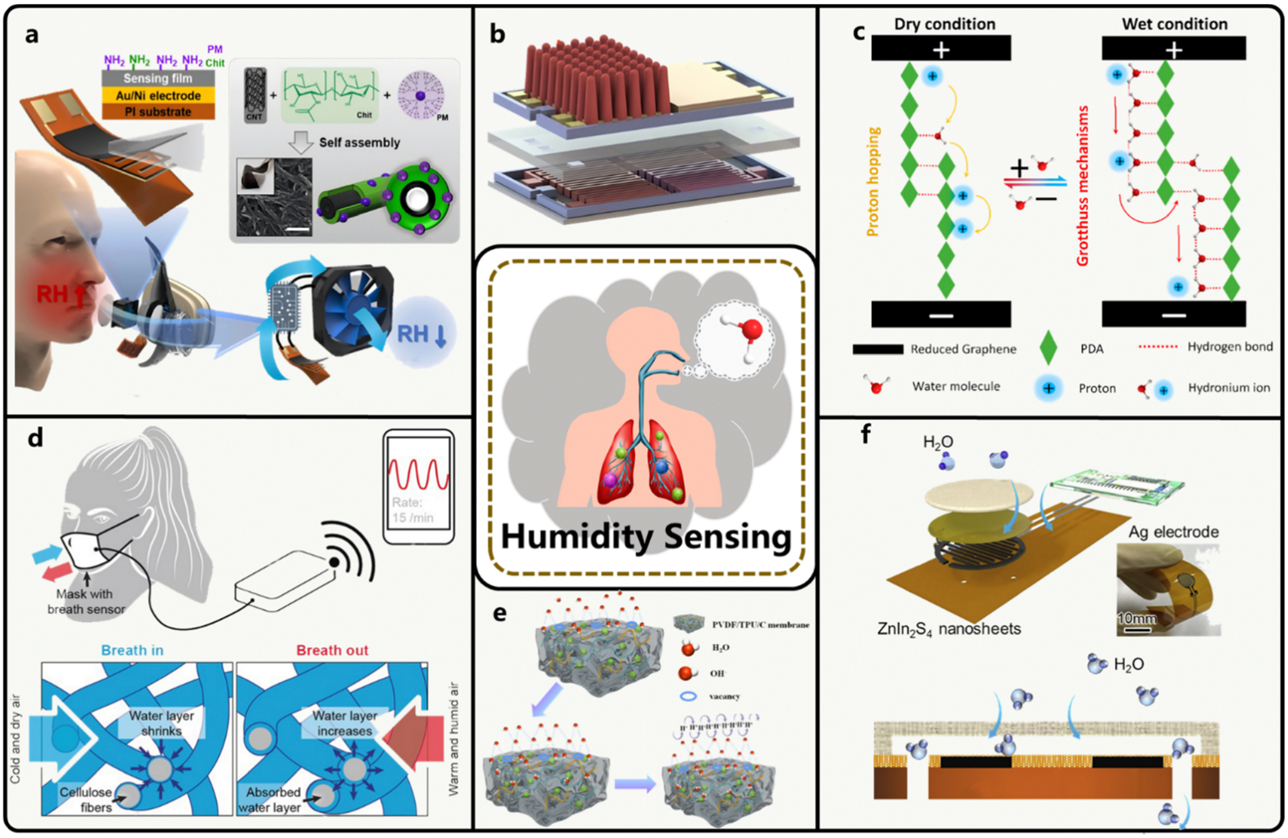

Fig. 7 Application of humidity sensors in masks. (a) A CNT-based, low-resistance, and flexible humidity sensor for respiration monitoring. Reproduced with permission from ref. 105. Copyright 2022 Nano Convergence. (b) A three-layer humidity sensor comprising a nano-forest-based sensing capacitor.[106] Copyright 2022 Microsystems & Nanoengineering. (c) Sensing mechanism of the GNCP humidity sensor.[107] Copyright 2018 Chemistry of Materials. (d) A simple paper-based sensor relying on changes in the humidity caused by breathing was fabricated. Reproduced with permission from ref. 108 Copyright 2016 Angewandte Chemie International Edition. (e) Schematic diagram of the sensor's humidity sensitivity mechanism.[109] Copyright 2024 Advanced Intelligent Systems. (f) Schematic illustration of the flexible ZIS humidity sensor.[110] Copyright 2022 iScience.

is made of highly sensitive nanofibers (NFs) with uniformly distributed thermochromic dyes, which enhance light transmittance by 10 to 30 times compared to conventional dense film sensors. This sensor allows for the real-time, visual monitoring of human respiratory temperature (Fig. 8(a)).[112]

In a different approach, the pyroelectric effect, which occurs when temperature fluctuations alter a material's polarization state, generating an electric charge on a specific surface, has been used to develop temperature sensors. Xue *et al.* integrated pyroelectric nanogenerators (PyNGs) into N95 masks, in which exhaled heat induces electric potentials at the electrodes, while inhalation-driven cooling generates a counter-current in the external circuit, converting respiratory temperature fluctuations into electrical signals (Fig. 8(b)).[113]

Similarly, Kim *et al.* also utilized the pyroelectric effect to develop a ZnO nanorod-modified paper (ZNR-paper) composite. This material undergoes *in situ* compressive and tensile strain during respiration, enhancing the pyroelectric effect. Additionally, it also promotes reactive oxygen species (ROS) generation, providing antibacterial and antiviral properties.[116]

Zhao *et al.* later proposed a wireless integrated sensing mask (WISE mask), which employs an ultrasensitive fiber temperature sensor. This system based on the proton transport properties of PAenhances the concentration of H^+ ions and improves proton mobility at elevated respiratory temperatures, enabling precise monitoring of body temperature and respiration (Fig. 8(c)).[114] Similarly, Xu *et al.* developed temperature sensors that track periodic respiratory patterns by detecting temperature variations during inhalation and exhalation. By integrating a peak detection algorithm with spline interpolation, the system enables real-time, low-cost, and energy-efficient respiratory monitoring, further advancing the capabilities of wearable health monitoring devices (Fig. 8(d)).[115] These innovations not only enhance the sensitivity and accuracy of monitoring systems but also contribute to the development of low-cost, real-time solutions that can provide early warnings of health or environmental changes, paving the way for more advanced and accessible healthcare technologies.

3.7 Other sensors

While most smart masks rely on conventional sensing mechanisms, novel sensors, such as transistors and dual-signal sensors, have also been integrated to enhance their functionality. Wang *et al.* developed polyvinyl alcohol (PVA)-based ion-gated transistors as biosensors for detecting trace viral proteins. The

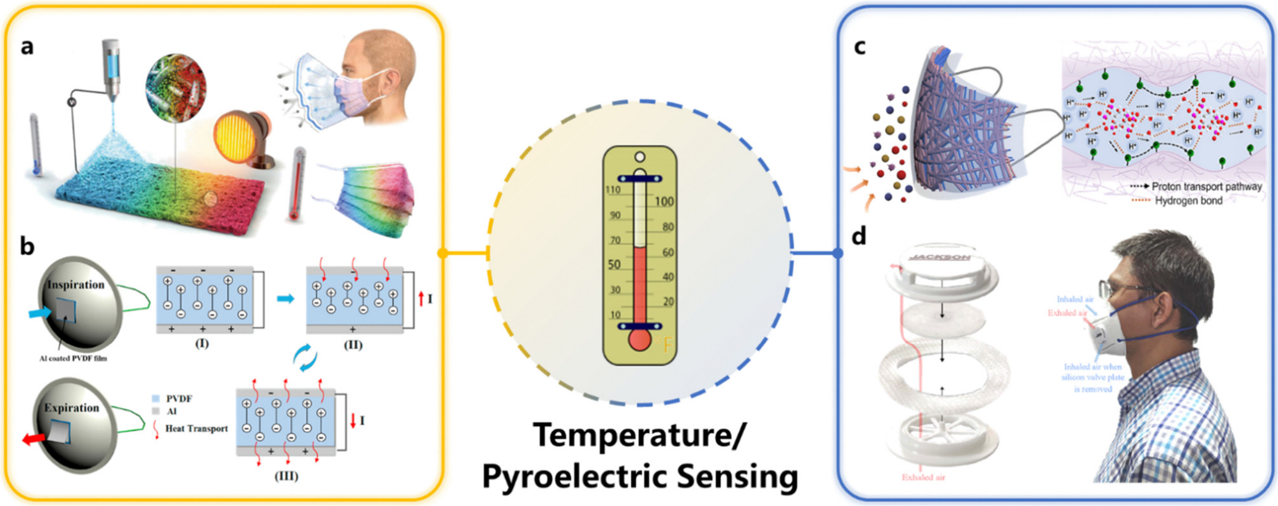

Fig. 8 Application of temperature/pyroelectric sensors in masks. (a) A porous nanofibre membrane-based thermochromic sensor.[112] Copyright 2022 Advanced Functional Materials. (b) Schematic of the principle of the PyNG which is driven by human respiratory system.[113] Copyright 2017 Nano Energy. (c) A wireless all-in-one sensory face mask (WISE mask) made of ultrasensitive fibrous temperature sensors. Reproduced with permission from ref. 114 Copyright 2023 Nano Letters. (d) KN95 mask with exhalation valve is constructed to detect temperature.[115] Copyright 2021 Sensors.

sensor utilizes a stretchable ionogel as the dielectric layer, which imparts a sensitive gating effect to the transistor. This allows the detection of viral proteins at low concentrations of 0.1–10 fg mL^{-1}. The smart mask can detect ultra-trace liquid samples (0.3 μL) and ultra-low concentration gas samples (0.1 fg mL^{-1}), enabling real-time detection of breath (Fig. 9(a)).[56] In a different approach, Chen *et al.* addressed the shortcomings of NH_3 sensors, such as low sensitivity and environmental susceptibility, by developing a visual NH_3 sensor and a dual-signal (optical and electrical) resistive NH_3 sensor. The visual sensor changes color from yellow-green to blue-green upon exposure to NH_3, while the resistive sensor exhibits resistance variations due to its nanostructures. The visual sensor is stable under diverse environmental conditions but less sensitive, whereas the resistive sensor offers high sensitivity, rapid response, and high resolution, although it is affected by humidity and temperature. Combining both sensors led to improved performance and more reliable NH_3 detection (Fig. 9(b)).[117]

Smart masks continue to evolve, and they are becoming multifunctional devices capable of monitoring multiple vital signs and biological parameters simultaneously, offering promising applications in healthcare, environmental monitoring, and food safety. Pan *et al.* proposed the "lab-on-mask" (LOM) concept, which integrates multiple sensors to monitor respiratory disease-related parameters such as heart rate (HR), blood pressure (BP), and blood oxygen saturation (SpO_2) (Fig. 9(c)).[118] In a similar vein, Dai *et al.* developed a self-powered multiparameter respiratory sensor (SMRS) that combines piezoelectric, pyroelectric, and gas-sensitive materials. One component of this sensor measures respiratory parameters, while another acts as a gas sensor for biomolecule (acetone) monitoring, enhancing diagnostic efficiency (Fig. 9(d)).[119] Zhang *et al.* designed BWAB masks with respiratory monitoring capabilities, featuring antimicrobial, waterproof, and high-breathability properties. The mask is composed of three layers: a silanized, self-cleaning water-repellent outer layer; an intermediate AgNP-based filter resistant to viral aerosols; and a respiratory sensor positioned between these layers (Fig. 9(e)).[120] In another development, Kim's group integrated machine-learning algorithms with a smart mask to monitor skin temperature, speech activity, breathing patterns, and mask-wearing status. This integration opens the door for more personalized and adaptive healthcare (Fig. 9(f)).[121] Additionally, Chen *et al.* explored the integration of resistive temperature sensors (R-TS) and capacitive respiratory sensors (C-RS) into smart masks. The R-TS detects temperature variations by increasing electron collisions and conductivity, while the C-RS modulates the electric field *via* gas molecules, enabling precise monitoring of vital signs.[122] As these devices become more sophisticated, their potential applications in healthcare, environmental monitoring, and even diagnostics continue to grow, providing significant opportunities for improving public health and safety.

3.8 Limitations of smart masks based on different sensing modalities

(i) Electrochemical sensor: electrodes are susceptible to contamination, as evidenced by instances in complex breathing environments where a variety of substances can be adsorbed on the electrode surface, thereby affecting their detection performance. Detection accuracy is significantly affected by environmental interference, where changes in temperature, humidity, and other environmental factors can alter the kinetic process of the electrode reaction, which in turn affects the accuracy of the detection results. Concurrently, the identification of the optimal humectant to function as an electrolyte remains a significant challenge, and the instability of electrolyte performance will compromise the overall performance of the sensor.

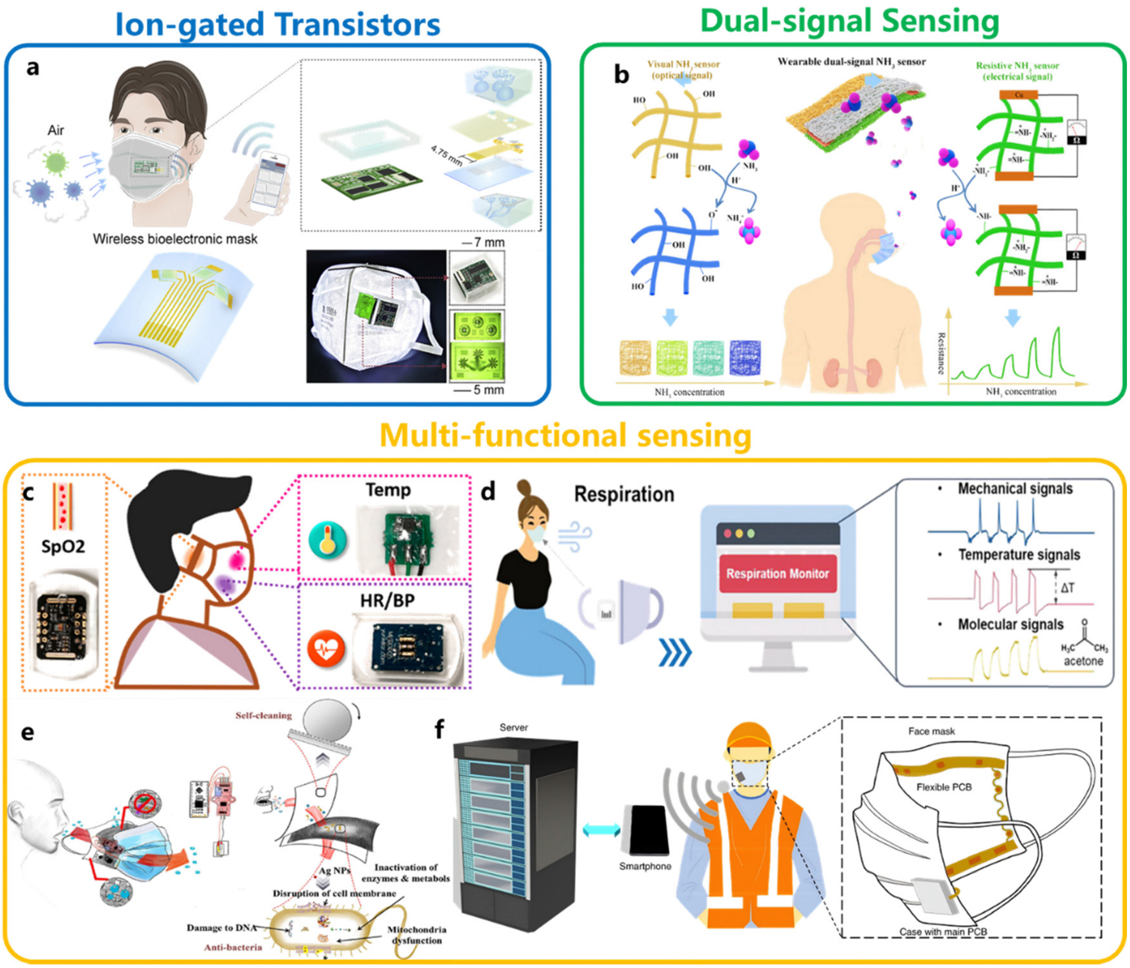

Fig. 9 Application of other sensors in masks. (a) Wearable bioelectronic facemasks integrated with ion-gated transistors.[56] Copyright 2022 Matter. (b) A wearable dual-signal NH_3 sensor for non-invasive monitoring of chronic kidney disease.[117] Copyright 2023 Langmuir. (c) Different sensors are embedded in the "Lab-on-Mask" (LOM). Reproduced with permission from ref. 118 Copyright 2020 ACS Materials Letters. (d) Diagram of the working process of the respiration monitoring system collecting mechanical signals, temperature signals, and molecular signals. Reproduced with permission from ref. 119 Copyright 2023 Advanced Materials Technologies. (e) The design of the high-breathable mask with self-cleaning, antibacterial, and breath monitoring features.[120] Copyright 2023 Chemical Engineering Journal. (f) A sensory face mask for monitoring signals related to infectious diseases, environmental conditions, and wear status of the face mask. Reproduced with permission from ref. 121 Copyright 2022 Nature Electronics.

(ii) Optical sensors: the process of fluorescence detection is susceptible to background fluorescence interference, and the presence of multiple fluorescent substances in the actual respiratory environment will interfere with the fluorescence signals of the target biomarkers, resulting in inaccurate detection results. Additionally, the detection range is limited, making it difficult to detect biomarkers outside the low or high concentration range accurately. The colorimetric method is limited in terms of sensitivity and precision for multi-component quantitative analysis, and it is difficult to accurately distinguish and determine the concentration of each substance when there are multiple biomarkers in the breath that need to be quantitatively analyzed simultaneously.

(iii) Piezoelectric sensors: it is important to note that the detection limit is relatively high, which can pose challenges in the effective detection of certain trace biomarkers or weak respiratory signal changes in breath. The sensor's performance is significantly influenced by the material used. Consequently, fluctuations in the material's performance directly impact the sensor's detection capability. Additionally, prolonged usage can lead to material fatigue and ageing, which can result in a decline in the sensor's effectiveness over time.

(iv) Bioaffinity recognition sensor: the number of receptors is limited, the types of biomarkers that can be detected are limited, and it is difficult to meet the demand for simultaneous detection of a variety of biomarkers; poor stability, the combination of biorecognition elements and target biomarkers is greatly affected by environmental factors such as temperature, humidity, etc., and it is difficult to ensure the repeatability and reliability of detection results under different environmental conditions.

(v) Humidity sensor: it is strongly affected by external environmental factors, and changes in ambient humidity can interfere with the detection of humidity changes caused by breathing, resulting in inaccurate detection results. Some humidity sensors have high power consumption, which increases the frequency of battery replacement and affects the user experience for smart masks that need to be worn for long periods of time and rely on battery power. Furthermore, humidity sensors utilising particular materials, such as paper-based sensors, are susceptible to issues including electrode cracking when folded, thereby reducing the sensor's lifespan.

(vi) Temperature sensors: these are also significantly affected by the external environment. Fluctuations in ambient temperature interfere with the accurate measurement of human respiratory temperature. Furthermore, the response speed of the temperature sensor is slow, which means that the rapid changes in the respiratory process of temperature signals cannot be accurately captured on time. This has a detrimental effect on the real-time monitoring of respiratory status. Conversely, in extreme environmental conditions characterised by elevated temperatures and humidity levels, the performance of these sensors may be severely compromised or even result in malfunction.

(vii) Other sensors: in the case of ion-gated transistors, for example, the preparation process is complex and costly, which is not conducive to large-scale production and application; the environmental operating requirements are harsh, and minor environmental changes can affect their performance in detecting biomarkers. In the case of dual-signal sensors, although these combine the advantages of two sensing modes, there is also a risk of mutual interference of the two sensing signals, which increases the complexity of signal processing and may lead to an increase in the error of detection results.

A smart mask, as a wearable device, involves core components that include various types of sensors, which can convert respiratory biological signals into readable data. It is widely used in the fields of health monitoring, disease diagnosis, and environmental monitoring. However, its development faces challenges such as sensor performance, wearing experience, and cost. To advance further, it is essential to make significant progress in these and other related areas.

4. Prospects and challenges

In this review, we explore the three key processes involved in real-time monitoring of human respiration using a smart mask: biomarker detection, biosensing process, and data signal output. We highlight the different types of biosensors in smart masks, including electrochemical, optical, piezoelectric, bioaffinity recognition, temperature sensors, and humidity sensors. In Table 2, we summarize the sensing methods, sensing materials, sensing process, and functionality of biosensors integrated into smart masks, which play crucial roles in detecting various biomarkers in real-time. Additionally, we analyzed the applications of these biosensors in disease diagnosis, healthcare, and environmental monitoring, showing how they are used to detect harmful gases, track respiratory biomarkers, and more. Finally, we discuss the advancements in these sensors and their prospects, focusing on innovations that aim to enhance their functionality, reliability, and applicability in diverse real-world contexts.

4.1 Prospects for smart masks

With the continuous advancement of technology and the growing emphasis on health monitoring, intelligent masks capable of real-time respiratory tracking are evolving at a remarkable pace.[129] These masks are on the verge of becoming an incredibly powerful tool, playing a pivotal role in health monitoring, providing protective function, and scene expansion in diverse fields.

4.1.1 Health monitoring. Smart masks represent a major advance in health monitoring, with the primary focus of the research being the implementation of biomarker detection. The primary focus of current research has been on integrating various sensing technologies to detect key biomarkers in exhaled breath. As shown in Table 2, these sensors employ different sensing materials and mechanisms, each optimized for specific biomarker detection with high sensitivity and selectivity. In particular, the integration of quantum nanostructures and electrospun materials has significantly enhanced sensor sensitivity.[130] Materials like TiO_2 and MXene have demonstrated improved detection capabilities. For example, simultaneous detection of the pH of nitric oxide (NO) and exhaled gas condensate (EBC) has been shown to have an impressive 92% accuracy in distinguishing between different asthma phenotypes.[33,34,131] This real-time, precise identification of disease-related characteristics is pivotal for the realization of personalized medical treatment. Furthermore, the incorporation of AI-driven anomaly detection algorithms has led to a substantial augmentation of the early warning capabilities of smart masks.[132] These algorithms are capable of meticulous analysis of breath volatile organic compound (VOC) patterns, enabling the identification of pre-symptomatic cases of SARS-CoV-2 two to three days before the onset of clinical symptoms.[91,92]

Looking ahead, future smart masks could potentially incorporate advanced nanomaterials, such as metal–organic frameworks (MOFs). These frameworks possess remarkably elevated surface areas and tunable pore sizes, which could be adapted to selectively capture and detect a more extensive array of disease-specific biomarkers with enhanced sensitivity. By modifying the structure of the sensor layer to accommodate these materials, for instance, through the creation of hierarchical porous structures, the masks could achieve more efficient mass transfer of analytes, further improving detection accuracy. This potential advancement could transform the early diagnosis of diseases such as lung cancer,[133–135] cardiovascular diseases,[136–138] and diabetes.[139,140] Additionally, it could play a crucial role in precision medicine by facilitating more targeted treatment strategies.

4.1.2 Protective function. In the field of protection, the advent of intelligent filtration systems in future smart masks is poised to transform the landscape of personal protection. Shape memory polymers (SMPs) are set to assume a pivotal function in the dynamic adjustment of pore size in response to environmental threats. In the event of pollutants or pathogens being encountered, SMPs can undergo a precise shape-shifting process, resulting in a narrowing of the pore size, thereby effectively blocking the smallest particles. In combination with a photocatalytic TiO_2 coating,[120] these masks can achieve a

Table 2 Summary of biosensors in smart masks for biomarker detection

Type of sensor	Sensing material	Sensing mechanism	Sensitivity	Selectivity	Response time	Stability	Ref.
Electrochemical	LSMO/Mica	Thermistor effect	—	—	0.1 s 0.7 s	1 weeks	123
	PP/$Ti_3C_2T_x$/PPy	Chemisorption and electron transfer	400 ppm	Responds to ethanol changes	49 s	13 days	51
	CeO_2@PANI	Oxygen vacancy adsorption	50 ppb	Responds to NH_3 changes	46 s	28 days	53
	$Ti_3C_2T_x$ MXene	Interlayer expansion	0.31 ppm	—	10 s	14 days	87
Optical	AgNCs	Ratiometric fluorescence response	0.8 ppb	Responds to H_2S changes	15 min	√	88
	AgNCs	Wettability differences	10^{-11}	High	30 s	24 h	89
	BPR, BPB, BCG, MR	Acid–base neutralization reactions	0.62 ppm	Anti-interference	≤60 s	√	93
	Porphyrazines, porphyrins, AuNPs, *etc.*	Acid–base reaction	—	Cross-response	75 min	√	92
Pressure	MEMS	Venturi effect	—	High	25 ms	√	124
	PVDF/GO	Piezoelectric and thermoelectric	10 Pa	—	—	√	102
	T-ZnO/PVDF	Piezoelectric/gas sensitive coupling	—	—	—	100 s	55
	CNT/PDMS	Piezoelectric	0.79 kPa^{-1} 0.088 kPa^{-1}	—	116.8 μs	√	125
Bioaffinity	PEDOT:PSS	Antibody–antigen binding	7 pfu m^{-1} 0.02 μg mL^{-1}	High	5 min	3 days	104
Humidity	AuNW	Resistive	11% RH	Cross-response	0.2 s	√	126
	Interdigitated electrodes and polyester threads	Capacitive	11.46% RH ∼ 27.41% RH and 29.79% RH ∼ 38.65% RH	—	—	80 min	127
	Nano-forest layer	Capacitive	40–90% RH	Responds to humidity changes	5 s	8 weeks	106
	Porous graphene	Resistive	—	Responds to humidity changes	—	√	128
Temperature	$(C_3H_6N_6{\cdot}CH_2O)_x$	Thermochromic	—	Responds to temperature changes	—	√	112
	PAN-PA/PP	Thermally induced proton transport	0.2 °C	Responds to temperature changes	1.2 s	√	114
	ZnO-paper	Pyroelectric	—	High	—	√	116
Transistors	PVA-IL	Ionic gating effect	0.1 fg mL^{-1}	High	10 min	14 days	56

99.99% viral inactivation rate while maintaining optimal breathability, thus ensuring protection and comfort.[141] Graphene-based materials have the potential to enhance the overall performance of the masks in terms of filtration and breathability. Furthermore, self-sterilizing mechanisms, such as the integration of UV-C LEDs into the mask structure,[113] represent a major leap forward in protection innovation.

In the future, the incorporation of advanced nanomaterials, such as metal–organic frameworks (MOFs), into smart masks holds potential. These frameworks possess remarkably elevated surface areas and tunable pore sizes, which could be adapted to selectively capture and detect a more extensive array of disease-specific biomarkers with enhanced sensitivity. By modifying the structure of the sensor layers to accommodate these materials, for instance, through the creation of hierarchical porous structures, the masks could achieve more efficient mass transfer of analytes, further improving detection accuracy. This potential advancement could transform the early diagnosis of diseases such as lung cancer, cardiovascular diseases, and diabetes. Additionally, it could play a crucial role in precision medicine by facilitating more targeted treatment strategies.

4.1.3 Scene expansion. Beyond healthcare, the potential applications of smart masks are rapidly being explored in a variety of contexts. In the field of occupational safety, MXene-based sensors have been utilised to detect noxious substances such as benzene in industrial environments,[86] thereby providing workers with real-time information about their working environment and aiding in the prevention of occupational diseases. In the sporting domain, the monitoring of lactate thresholds through EBC analysis can assist athletes in optimizing their performance and ensuring they train at an appropriate intensity.[83]

Looking ahead, the development of smart masks with modular structure is expected, allowing for easy customization based on specific applications. For sports applications,[142] sensors could be integrated to monitor not only lactate thresholds but also other parameters such as heart rate variability, oxygen saturation, and muscle fatigue markers. The use of flexible and stretchable materials, such as elastomeric polymers with embedded sensors, would enable the mask to conform to the body's movements during exercise without compromising functionality. In the context of environmental monitoring,[31,34,118] the development of materials with enhanced gas-sensing capabilities, such as doped semiconductors, is a promising area for exploration. The incorporation of such materials into the mask structure could enhance the detection of harmful gases and volatile organic compounds, thereby ensuring the provision of more accurate and timely environmental data. Furthermore, the incorporation of energy-harvesting technologies, such as piezoelectric materials that generate electricity from the wearer's movements, has the potential to render smart masks self-sufficient, thus eliminating the requirement for external power sources. Currently, there are FDA-approved smart masks available on the market. These masks outperform N95 masks in terms of filtration efficiency, such as the Crosstex SecureFit and Ultramax UltraOne, which offer filtration efficiencies of 99.9% and 99.97%, respectively. They also provide improved fit, reusability, and additional smart features like active ventilation and airflow regulation, as shown in Table 3. These masks are designed with medical-grade materials, such as silicone face seals, and are rechargeable with replaceable filters. The future of smart masks is promising, as they are likely to become a part of daily life due to their enhanced functionality and adaptability to various applications.

In conclusion, the development of smart masks is opening up vast possibilities for health monitoring and protection. By focusing on the development of advanced materials and innovative structural designs, smart masks are poised not only to enhance their current capabilities but also to redefine the boundaries of wearable technology, thereby bringing about a profound impact on people's daily lives and health management. Additionally, features such as self-powering,[14] thermal management,[143–145] and antibacterial and antiviral properties are gradually being integrated into smart masks. The advancement of smart masks is expanding the possibilities for health monitoring, propelling wearable technology into a new era.

4.2 Limitations and challenges of smart masks

Despite the bright future of smart masks, they face challenges in device design, performance enhancement, and market production, and require further research and development:

4.2.1 Comfort and safety of mask wear. Achieving accurate biomarker detection necessitates the sensor being in full contact with the user's respiratory airflow. However, the biosensor's integration into the mask may compromise the comfort and fit of the mask, potentially leading to impaired respiration and skin discomfort. To illustrate this point, consider the impact of smart mask integration on the mask's structural integrity. The alteration of the mask's internal structure can potentially compromise its original fit, resulting in users experiencing breathlessness during wear, akin to the sensation of breathing in a confined environment. Furthermore, the prolonged use of such masks has the potential to induce adverse cutaneous reactions, including pruritus, erythema, and tumefaction, among others, as a consequence of direct or indirect contact between the sensor and the epidermis.[121,122]

A further salient issue pertains to the safety of smart masks. The inner layer of the mask comes into direct contact with the user's skin, nose, and mouth, ranking among the most vulnerable regions of the human body. In the event of sensor damage, there is a significant risk to human safety.[121] During the manufacturing process, various conditions may be present, including mask damage from daily folding or extrusion, or gradual circuit exposure over time. In the case of some smart masks with more complex circuit design, repeated bending can cause the internal electrode material to break, which can affect the normal functioning of the sensor and lead to current leakage, potentially causing harm to the user. Consequently, during the design phase of smart masks, it is imperative to meticulously consider these potential safety hazards and formulate pragmatic preventive measures to ensure user safety.

4.2.2 Sensor performance and responsiveness. The sensitivity and selectivity of the sensor are critical for the accurate detection of respiratory biomarkers.[70,104] In the context of ammonia detection, there is a possibility of a non-specific reaction between the sensor by ammonia and nitric oxide, resulting in interference with the sensor's ability to accurately determine ammonia concentration. This can lead to biased detection results. Consequently, to ensure the accuracy of detection results, it is imperative to develop sensors with extremely high sensitivity, thereby enabling precise recognition of target biomarkers and effective avoidance of bias caused by the presence of interfering substances.

Table 3 Performance of FDA-approved smart masks *vs.* regular masks

Comparison dimension	Regular medical mask (*e.g.*, N95)	Crosstex securefit	Ultramasx ultraone
Filtration efficiency	95%	99.9%	99.97%
Filter particles	≥0.3 μm	≥0.1 μm	≥0.3 μm
Protective properties	Suitable for everyday low-risk environments	Suitable for medical/haze scenarios	Active ventilation improves protection efficiency
Breathability	Passive filtration, high breathing resistance	Dual seal design, but no active ventilation	Active electric turbo ventilation
Smart features	×	×	Active airflow regulation, rechargeable
Sustainability	Single-use	Reusable	Rechargeable + replaceable filter
Fit	Single nose strip design	Double Seal Shape Control Strip	Medical grade silicone face seal
Material safety	May contain latex/irritants	Anti-allergic fiber inner layer	Silicone tested for biocompatibility
Prices	\$0.5–2 per piece	∼\$1.5–5 per piece	∼\$150–200 (device) + \$20–30 per filter

Concurrently, the responsiveness of the sensors must be enhanced. During respiration, many biomarkers diffuse rapidly, or their half-life time is very short and easy to disappear.[56] If the biosensor's response performance is not high enough, it will greatly affect the detection results. Some biomarkers diffuse into the surrounding environment within seconds of exhalation; if the sensor cannot detect them within this very short period of time, the optimum time for detection will be missed. Furthermore, the electrodes of the sensor will deteriorate over time, and the internal components will deteriorate, making the sensor less responsive and ultimately unable to provide the user with reliable detection data consistently.

4.2.3 Cost and market production. At present, the research and production costs of smart masks are relatively high, which considerably limits the large-scale development and production of smart masks. The fabrication of sensors capable of detecting multiple biomarkers necessitates the utilization of nanomaterials, special electrode materials, and other costly components. The manufacturing process is intricate and requires strict control of the production environment and process parameters, which further increases the production cost.[51,87] The development of sophisticated data processing systems necessitates considerable human, material, and financial resources. The generation of substantial testing data by the smart mask necessitates rapid and precise analysis and processing, which in turn requires the development of specialized data processing algorithms and software, as well as high-performance computing equipment. The material and process costs of masks are likewise not to be underestimated. To realize the various functions of smart masks, it is necessary to use some special materials, such as materials with good air permeability, filtration and biocompatibility, and at the same time, it is also necessary to use more delicate and complex technology in the manufacturing process to ensure the perfect combination of sensors and masks, which will lead to a significant increase in the production cost of masks.

Author contributions

Jiahui Liang: conceptualization, visualization, and writing – original draft. Conghui Liu: funding acquisition, and writing – review & editing. Tailin Xu: supervision, funding acquisition, and writing – review & editing.

Data availability

No primary research results, software or code have been included and no new data were generated or analysed as part of this review.

Conflicts of interest

There are no conflicts to declare.

Acknowledgements

We acknowledge funding from the Guangdong University Student Science and Technology Innovation Cultivation Special Fund Support Project (pdjh2024b323), Shenzhen Medical Research Fund (A2403003), Shenzhen Science and Technology Program (JCYJ20240813142503006), and Shenzhen Key Laboratory for Nano-Biosensing Technology (ZDSYS20210112161400001).

Notes and references

1 W. Deng, Y. Sun, X. Yao, K. Subramanian, C. Ling, H. Wang, S. S. Chopra, B. B. Xu, J. X. Wang, J. F. Chen, D. Wang, H. Amancio, S. Pramana, R. Ye and S. Wang, *Adv. Sci.*, 2021, **9**, 2102189.
2 L. H. Kwong, R. Wilson, S. Kumar, Y. S. Crider, Y. Reyes Sanchez, D. Rempel and A. Pillarisetti, *ACS Nano*, 2021, **15**, 5904–5924.
3 C. D. Zangmeister, J. G. Radney, E. P. Vicenzi and J. L. Weaver, *ACS Nano*, 2020, **14**, 9188–9200.
4 H. Ueki, Y. Furusawa, K. Iwatsuki-Horimoto, M. Imai, H. Kabata, H. Nishimura and Y. Kawaoka, *mSphere*, 2020, **5**(5), 5, DOI: **10.1128/msphere.00637-20**.
5 B. Hu, *TrAC, Trends Anal. Chem.*, 2022, **151**, 116600.
6 J. Howard, A. Huang, Z. Li, Z. Tufekci, V. Zdimal, H.-M. van der Westhuizen, A. von Delft, A. Price, L. Fridman, L.-H. Tang, V. Tang, G. L. Watson, C. E. Bax, R. Shaikh, F. Questier, D. Hernandez, L. F. Chu, C. M. Ramirez and A. W. Rimoin, *Proc. Natl. Acad. Sci. U. S. A.*, 2021, **118**, e2014564118.
7 Vibhuti, N. Jindal, H. Singh and P. S. Rana, *Multimed. Tools Appl.*, 2022, **81**, 40013–40042.
8 C. Matuschek, F. Moll, H. Fangerau, J. C. Fischer, K. Zänker, M. van Griensven, M. Schneider, D. Kindgen-Milles, W. T. Knoefel, A. Lichtenberg, B. Tamaskovics, F. J. Djiepmo-Njanang, W. Budach, S. Corradini, D. Häussinger, T. Feldt, B. Jensen, R. Pelka, K. Orth, M. Peiper, O. Grebe, K. Maas, P. A. Gerber, A. Pedoto, E. Bölke and J. Haussmann, *Eur. J. Med. Res.*, 2020, **25**, 32.
9 L. W. Chan, M. N. Anahtar, T.-H. Ong, K. E. Hern, R. R. Kunz and S. N. Bhatia, *Nat. Nanotechnol.*, 2020, **15**, 792–800.
10 N. M. Grob, M. Aytekin and R. A. Dweik, *J. Breath Res.*, 2008, **2**, 037004.
11 X. Jin, C. Liu, T. Xu, L. Su and X. Zhang, *Biosens. Bioelectron.*, 2020, **165**, 112412.
12 M. Adeel, Y. Cotur, A. Naik, L. Gonzalez-Macia and F. Güder, *Nat. Electron.*, 2022, **5**, 719–720.
13 A. A. Smith, R. Li and Z. T. H. Tse, *Sci. Rep.*, 2023, **13**, 4998.
14 U. Erturun, C. Yalim and J. E. West, *Electron. Lett.*, 2024, **60**, e13241.
15 G. Liu, J. Nie, C. Han, T. Jiang, Z. Yang, Y. Pang, L. Xu, T. Guo, T. Bu, C. Zhang and Z. L. Wang, *ACS Appl. Mater. Interfaces*, 2018, **10**, 7126–7133.
16 X. Y. D. Soo, S. Wang, C. C. J. Yeo, J. Li, X. P. Ni, L. Jiang, K. Xue, Z. Li, X. Fei, Q. Zhu and X. J. Loh, *Sci. Total Environ.*, 2022, **807**, 151084.

17 S. Choi, H. Jeon, M. Jang, H. Kim, G. Shin, J. M. Koo, M. Lee, H. K. Sung, Y. Eom, H. S. Yang, J. Jegal, J. Park, D. X. Oh and S. Y. Hwang, *Adv. Sci.*, 2021, **8**, 2003155.
18 L. Huang, S. Xu, Z. Wang, K. Xue, J. Su, Y. Song, S. Chen, C. Zhu, B. Z. Tang and R. Ye, *ACS Nano*, 2020, **14**, 12045–12053.
19 Q. Li, Y. Yin, D. Cao, Y. Wang, P. Luan, X. Sun, W. Liang and H. Zhu, *ACS Nano*, 2021, **15**, 11992–12005.
20 R. He, J. Li, M. Chen, S. Zhang, Y. Cheng, X. Ning and N. Wang, *J. Hazard. Mater.*, 2022, **428**, 128239.
21 M. Abulikemu, B. E. A. Tabrizi, S. M. Ghobadloo, H. M. Mofarah and G. E. Jabbour, *ACS Appl. Nano Mater.*, 2021, **5**, 309–317.
22 J. E. Tavis, G. Borkow, S. S. Zhou, T. Page and J. Gabbay, *PLoS One*, 2010, **5**, e11295.
23 B. Ghatak, S. Banerjee, S. B. Ali, R. Bandyopadhyay, N. Das, D. Mandal and B. Tudu, *Nano Energy*, 2021, **79**, 105387.
24 M. B. Kulkarni, S. Rajagopal, B. Prieto-Simón and B. W. Pogue, *Talanta*, 2024, **272**, 125817.
25 J. F. Wang, Z. B. Zhang, W. J. Li, Z. B. Wang and Ieee, Shenzhen, Peoples R China, 2024.
26 M. H. Fakir and J. K. Kim, *Build. Environ.*, 2022, **207**, 108507.
27 A. Mutti, M. Corradi, M. Goldoni, M. V. Vettori, A. Bernard and P. Apostoli, *Chest*, 2006, **129**, 1288–1297.
28 J. H. J. Sng, S. Prazakova, P. S. Thomas and C. Herbert, *COPD*, 2017, **14**, 238–244.
29 M. K. Al-Ali and P. H. Howarth, *Saudi. Med. J.*, 2001, **22**, 249–253.
30 S. Kobayashi, M. Hanagama, M. Ishida, M. Ono, H. Sato and M. Yanai, *Respir. Invest.*, 2021, **59**, 364–366.
31 S. Cheng, D. Enserro, V. Xanthakis, L. M. Sullivan, J. M. Murabito, E. J. Benjamin, J. F. Polak, C. J. O'Donnell, P. A. Wolf, G. T. O'Connor, J. F. Keaney and R. S. Vasan, *Eur. Heart J.*, 2014, **35**, 2980–2987.
32 S. Cheng, A. Lyass, J. M. Massaro, G. T. O'Connor, J. F. Keaney and R. S. Vasan, *Circulation*, 2010, **122**, 1470–1477.
33 S. Ghosh and S. C. Erzurum, *Biochim. Biophys. Acta, Gen. Subj.*, 2011, **1810**, 1008–1016.
34 C. Krantz, C. Janson, K. Alving and A. Malinovschi, *Nitric oxide*, 2021, **106**, 1–8.
35 P. Paredi, S. A. Kharitonov and P. J. Barnes, *Am. J. Respir. Crit. Care Med.*, 2000, **162**, 1450–1454.
36 M. Hosseinzadeh Fakhr, I. Lopez Carrasco, D. Belyaev, J. Kang, Y. Shin, J.-S. Yeo, W.-G. Koh, J. Ham, A. Michaelis, J. Opitz and N. Beshchasna, *Biosens. Bioelectron.: X*, 2024, **19**, 100503.
37 J. Chandrasekar, M. Venkatesan, T. W. Sun, Y. C. Hsu, Y. H. Huang, W. W. Chen, M. H. Chen, M. L. Tsai, J. Y. Chen, J. H. Lin, Y. Zhou and C. C. Kuo, *Mater. Horiz.*, 2024, **11**, 1395–1413.
38 J. V. Vaghasiya, C. C. Mayorga-Martinez and M. Pumera, *npj Flexible Electron.*, 2023, **7**, 26.
39 P. C. Moura, M. M. Raposo and V. Vassilenko, *Biomed. J.*, 2023, **46**, 100623.
40 Y. Xu and J. S. Zhang, *ASHRAE J.*, 2011, **53**, 121–125.
41 M. Phillips, R. N. Cataneo, J. Greenberg, R. Grodman, R. Gunawardena and A. Naidu, *Eur. Respir. J.*, 2003, **21**, 48–51.
42 Y. B. Lee and C. K. Kang, *Appl. Sci.*, 2021, **11**, 1161.
43 S. X. L. Luo and T. M. Swager, *ACS Nano*, 2023, **18**, 364–372.
44 M. Navratil, D. Plavec, D. Erceg, S. B. Lokas, J. Zivkovic and M. Turkalj, *J. Asthma*, 2015, **52**, 437–446.
45 K. S. Zeller, H. Johansson, T. O. Lund, N. N. Kristensen, E. L. Roggen and M. Lindstedt, *Toxicol. In Vitro*, 2018, **46**, 155–162.
46 S. T. Moein, S. M. Hashemian, B. Mansourafshar, A. Khorram-Tousi, P. Tabarsi and R. L. Doty, *Int. Forum Allergy Rhinol.*, 2020, **10**, 944–950.
47 D. Kim, J. Lee, M. K. Park and S. H. Ko, *Commun. Mater.*, 2024, **5**, 41.
48 Z. Sun, W. Guo, C.-K. Chan, L. Jin, S. M. Griffith, J. Z. Yu and W. Chan, *Chem. Res. Toxicol.*, 2022, **35**, 1604–1613.
49 W. Chan, L. Jin, Z. Sun, S. M. Griffith and J. Z. Yu, *Environ. Sci. Technol.*, 2021, **55**, 5128–5135.
50 W. Chan, W. Guo and J. Z. Yu, *Anal. Chem.*, 2021, **93**, 13912–13918.
51 G. Wu, H. Du, K. Pakravan, W. Kim, Y. L. Cha, M. Beidaghi, X. Zhang, X. Pan and D.-J. Kim, *Carbon*, 2024, **216**, 118565.
52 I. Jeerapan, W. Sangsudcha and P. Phokhonwong, *Sens. Bio-Sens. Res.*, 2022, **38**, 100525.
53 C. Wang, Y. Cai, W. Zhou, P. Chen, L. Xu, T. Han, Y. Hu, X. Xu, B. Liu and X. Yu, *ACS Appl. Mater. Interfaces*, 2022, **14**, 12630–12639.
54 G. Wu, H. Du, D. Lee, Y. L. Cha, W. Kim, X. Zhang and D.-J. Kim, *ACS Appl. Mater. Interfaces*, 2022, **14**, 56056–56064.
55 Y. Lin, Z. Long, S. Liang, T. Zhong and L. Xing, *J. Phys. D: Appl. Phys.*, 2022, **55**, 224001.
56 B. Wang, D. Yang, Z. Chang, R. Zhang, J. Dai and Y. Fang, *Matter*, 2022, **5**, 4347–4362.
57 J. Min, J. Tu, C. Xu, H. Lukas, S. Shin, Y. Yang, S. A. Solomon, D. Mukasa and W. Gao, *Chem. Rev.*, 2023, **123**, 5049–5138.
58 K. Mahato and J. S. Wang, *Sens. Actuators, B*, 2021, **344**, 130178.
59 D. Moravcová, R. Soukup and A. Hamácek, Jetrichovice, Czech Republic, 2018.
60 E. Bilbao, O. Garate, T. R. Campos, M. Roberti, M. Mass, A. Lozano, G. Longinotti, L. Monsalve and G. Ybarra, *Chemosensors*, 2023, **11**, 244.
61 Y. Sekine, S. B. Kim, Y. Zhang, A. J. Bandodkar, S. Xu, J. Choi, M. Irie, T. R. Ray, P. Kohli, N. Kozai, T. Sugita, Y. Wu, K. Lee, K.-T. Lee, R. Ghaffari and J. A. Rogers, *Lab Chip*, 2018, **18**, 2178–2186.
62 Z. Zhou, T. Shu, Y. Sun, H. Si, P. Peng, L. Su and X. Zhang, *Biosens. Bioelectron.*, 2021, **192**, 113530.
63 O. V. Monogarova, K. V. Oskolok and V. V. Apyari, *J. Anal. Chem.*, 2018, **73**, 1076–1084.
64 N. Nikitina, E. Reshetnyak, V. Shevchenko and Y. Zhitnyakovskaya, *Stud. Univ. Babes-Bolyai, Chem.*, 2011, **56**, 265–282.
65 A. A. Chaplenko, O. V. Monogarova, K. V. Oskolok and A. V. Garmay, *Mosc. Univ. Chem. Bull.*, 2022, **77**, 61–67.
66 J. F. Tressler, S. Alkoy and R. E. Newnham, *J. Electroceram.*, 1998, **2**, 257–272.

67 D. H. Han and L. H. Kang, *Funct. Compos. Struct.*, 2020, **2**, 025002.
68 E. J. Curry, K. Ke, M. T. Chorsi, K. S. Wrobel, A. N. Miller, A. Patel, I. Kim, J. L. Feng, L. X. Yue, Q. Wu, C. L. Kuo, K. W. H. Lo, C. T. Laurencin, H. Ilies, P. K. Purohit and T. D. Nguyen, *Proc. Natl. Acad. Sci. U. S. A.*, 2018, **115**, 909–914.
69 X. He, T. Xu, Z. Gu, W. Gao, L.-P. Xu, T. Pan and X. Zhang, *Anal. Chem.*, 2019, **91**, 4296–4300.
70 L. Gutiérrez-Gálvez, N. Seddaoui, L. Fiore, L. Fabiani, T. García-Mendiola, E. Lorenzo and F. Arduini, *ACS Sens.*, 2024, **9**, 4047–4057.
71 J. Majewski, *Metrol. Meas. Syst.*, 2017, **24**, 607–616.
72 J. Boudaden, M. Steinmassl, H. E. Endres, A. Drost, I. Eisele, C. Kutter and P. Müller-Buschbaum, *Sensors*, 2018, **18**, 1516.
73 J. Kim, J. H. Cho, H. M. Lee and S. M. Hong, *Sensors*, 2021, **21**, 1974.
74 A. Somov, E. Kovalska, A. Baldycheva and Ieee, Electr Network, 2020.
75 R. P. Liu, L. He, M. J. Cao, Z. C. Sun, R. Q. Zhu and Y. Li, *Front. Chem.*, 2021, **9**, 539678.
76 B. A. Kuzubasoglu and S. K. Bahadir, *Sens. Actuators*, 2020, **315**, 112282.
77 T. Bose, S. Bandyopadhyay, S. Kumar, A. Bhattacharyya, A. Pal and Ieee, London, England, 2016.
78 P. Munster, J. Vojtech, T. Horvath, O. Havlis, P. Hanak, M. Cucka and M. Filka, Vienna, Austria, 2016.
79 A. Manchanda, K. Lee, G. D. Poznanski and A. Hassani, *Sensors*, 2023, **23**, 1711.
80 V. Ratnayake Mudiyanselage, K. Lee and A. Hassani, *Sensors*, 2022, **22**, 9463.
81 V. Ramji, M. Hssayeni, M. A. Burack, B. Ghoraani and Ieee, Orlando, FL, 2017.
82 S. Begum, S. Barua and M. U. Ahmed, *Sensors*, 2014, **14**, 11770–11785.
83 W. Z. Heng, S. K. Yin, J. H. Min, C. R. Wang, H. Han, E. S. Sani, J. H. Li, Y. Song, H. B. Rossiter and W. Gao, *Science*, 2024, **385**, 954–961.
84 D. Maier, E. Laubender, A. Basavanna, S. Schumann, F. Güder, G. A. Urban and C. Dincer, *ACS Sens.*, 2019, **4**, 2945–2951.
85 Y. Cao, H. Shi, Y. Zheng, Z. Tan, Z. Xie, C. Zhang and Z. Chen, *Sens. Actuators, B*, 2023, **393**, 134189.
86 X. Li, Z. An, Y. Lu, J. Shan, H. Xing, G. Liu, Z. Shi, Y. He, Q. Chen, R. P. S. Han, D. Wang, J. Jiang, F. Zhang and Q. Liu, *Adv. Mater. Technol.*, 2021, **7**, 2100872.
87 X. Li, J. Pan, Y. Wu, H. Xing, Z. An, Z. Shi, J. Lv, F. Zhang, J. Jiang, D. Wang, R. P. S. Han, B. Su, Y. Lu and Q. Liu, *Biosens. Bioelectron.*, 2023, **222**, 114945.
88 S. Zhang, J. Wang, Y.-J. Zeng and T. Xu, *ACS Sens.*, 2024, **9**, 6638–6645.
89 C. Chen, J. Liu, J. Lu, Y. Wang, J. Zhai, H. Zhao and N. Lu, *ACS Sens.*, 2024, **9**, 3680–3688.
90 P. Escobedo, M. D. Fernández-Ramos, N. López-Ruiz, O. Moyano-Rodríguez, A. Martínez-Olmos, I. M. Pérez de Vargas-Sansalvador, M. A. Carvajal, L. F. Capitán-Vallvey and A. J. Palma, *Nat. Commun.*, 2022, **13**, 72.
91 P. Q. Nguyen, L. R. Soenksen, N. M. Donghia, N. M. Angenent-Mari, H. de Puig, A. Huang, R. Lee, S. Slomovic, T. Galbersanini, G. Lansberry, H. M. Sallum, E. M. Zhao, J. B. Niemi and J. J. Collins, *Nat. Biotechnol.*, 2021, **39**, 1366–1374.
92 M. M. Bordbar, H. Samadinia, A. Hajian, A. Sheini, E. Safaei, J. Aboonajmi, F. Arduini, H. Sharghi, P. Hashemi, H. Khoshsafar, M. Ghanei and H. Bagheri, *Sens. Actuators, B*, 2022, **369**, 132379.
93 J. Wang, Z. Zhou, Y. Luo, T. Xu, L. Xu and X. Zhang, *Anal. Chem.*, 2023, **96**, 381–387.
94 A. Vaquer, A. Alba-Patiño, C. Adrover-Jaume, S. M. Russell, M. Aranda, M. Borges, J. Mena, A. del Castillo, A. Socias, L. Martín, M. M. Arellano, M. Agudo, M. Gonzalez-Freire, M. Besalduch, A. Clemente, E. Barón and R. de la Rica, *Sens. Actuators, B*, 2021, **345**, 130347.
95 Z. Jin, A. Jorns, W. Yim, R. Wing, Y. Mantri, J. Zhou, J. Zhou, Z. Wu, C. Moore, W. F. Penny and J. V. Jokerst, *Anal. Chem.*, 2021, **93**, 11025–11032.
96 H. He, J. Guo, B. Illés, A. Géczy, B. Istók, V. Hliva, D. Török, J. G. Kovács, I. Harmati and K. Molnár, *Nano Energy*, 2021, **89**, 106418.
97 A. Vázquez-López, J. S. del Río Saez, J. de la Vega, X. Ao and D.-Y. Wang, *ACS Sens.*, 2023, **8**, 1684–1692.
98 K. Zhang, Z. Li, J. Zhang, D. Zhao, Y. Pi, Y. Shi, R. Wang, P. Chen, C. Li, G. Chen, I. M. Lei and J. Zhong, *ACS Sens.*, 2022, **7**, 3135–3143.
99 L. Yang, H. Wang, W. Yuan, Y. Li, P. Gao, N. Tiwari, X. Chen, Z. Wang, G. Niu and H. Cheng, *ACS Appl. Mater. Interfaces*, 2021, **13**, 60531–60543.
100 L. Gao, Y. Liu, Z. Wang, Y. He, P. Wang, Y. Li, L. Li, X. Yu and J. Yu, *IEEE Trans. Electron Devices*, 2021, **68**, 5765–5772.
101 C. Ding, Y. Liu, P. Xie, J. Lan, Y. Yu, X. Fu, X. Yang and W.-H. Zhong, *J. Mater. Chem. A*, 2021, **9**, 13143–13150.
102 K. Roy, S. K. Ghosh, A. Sultana, S. Garain, M. Xie, C. R. Bowen, K. Henkel, D. Schmeiβer and D. Mandal, *ACS Appl. Nano Mater.*, 2019, **2**, 2013–2025.
103 J. Zhong, Z. Li, M. Takakuwa, D. Inoue, D. Hashizume, Z. Jiang, Y. Shi, L. Ou, M. O. G. Nayeem, S. Umezu, K. Fukuda and T. Someya, *Adv. Mater.*, 2021, **34**, 2107758.
104 Q. Xue, X. Kan, Z. Pan, Z. Li, W. Pan, F. Zhou and X. Duan, *Biosens. Bioelectron.*, 2021, **186**, 113286.
105 H.-S. Kim, J.-H. Kang, J.-Y. Hwang and U. S. Shin, *Nano Converg.*, 2022, **9**, 35.
106 G. Chen, R. Guan, M. Shi, X. Dai, H. Li, N. Zhou, D. Chen and H. Mao, *Microsyst. Nanoeng.*, 2022, **8**, 44.
107 J. He, P. Xiao, J. Shi, Y. Liang, W. Lu, Y. Chen, W. Wang, P. Théato, S.-W. Kuo and T. Chen, *Chem. Mater.*, 2018, **30**, 4343–4354.
108 F. Güder, A. Ainla, J. Redston, B. Mosadegh, A. Glavan, T. J. Martin and G. M. Whitesides, *Angew. Chem., Int. Ed.*, 2016, **55**, 5727–5732.
109 Y. Wang, X. Qi, L. Chen, Y. Cheng, Z. Mu, X. Gu, S. Li, Y. Song, X. He and S. Huang, *Adv. Intell. Syst.*, 2024, 2400537, DOI: 10.1002/aisy.202400537,.

110 S. Honda, H. Hara, T. Arie, S. Akita and K. Takei, *iScience*, 2022, **25**, 104163.
111 Z. Duan, Y. Jiang, M. Yan, S. Wang, Z. Yuan, Q. Zhao, P. Sun, G. Xie, X. Du and H. Tai, *ACS Appl. Mater. Interfaces*, 2019, **11**, 21840–21849.
112 D. H. Kim, J. Bae, J. Lee, J. Ahn, W. T. Hwang, J. Ko and I. D. Kim, *Adv. Funct. Mater.*, 2022, **32**, 2200463.
113 H. Xue, Q. Yang, D. Wang, W. Luo, W. Wang, M. Lin, D. Liang and Q. Luo, *Nano Energy*, 2017, **38**, 147–154.
114 T. Zhao, X. Xiao, Y. Wu, J. Ma, Y. Li, C. Lu, C. Shokoohi, Y. Xu, X. Zhang, Y. Zhang, G. Ge, G. Zhang, J. Chen and Y. Zeng, *Nano Lett.*, 2023, **23**, 8960–8969.
115 Y. Xu, Q. Li, Z. Tang, J. Liu and B. Xiang, *Sensors*, 2021, **21**, 6698.
116 M. J. Kim, Z. Song, C. K. Lee, T. G. Yun, J. Y. Noh, M. K. Park, D. Yong, M. J. Kang and J. C. Pyun, *Small*, 2022, **19**, 2200712.
117 H. Chen, J. Chen, Y. Liu, B. Li, H. Li, X. Zhang, C. Lv and H. Dong, *Langmuir*, 2023, **39**, 3420–3430.
118 L. Pan, C. Wang, H. Jin, J. Li, L. Yang, Y. Zheng, Y. Wen, B. H. Tan, X. J. Loh and X. Chen, *ACS Mater. Lett.*, 2020, **2**, 1178–1181.
119 J. Dai, J. Meng, X. Zhao, W. Zhang, Y. Fan, B. Shi and Z. Li, *Adv. Mater. Technol.*, 2023, **8**, 2201535.
120 F. Zhang, J. Lin, M. Yang, Y. Wang, Z. Ye, J. He, J. Shen, X. Zhou, Z. Guo, Y. Zhang and B. Wang, *Chem. Eng. J.*, 2023, **466**, 143150.
121 J.-H. Kim, C. Marcus, R. Ono, D. Sadat, A. Mirzazadeh, M. Jens, S. Fernandez, S. Zheng, T. Durak and C. Dagdeviren, *Nat. Electron.*, 2022, **5**, 794–807.
122 S. Chen, G. Qian, B. Ghanem, Y. Wang, Z. Shu, X. Zhao, L. Yang, X. Liao and Y. Zheng, *Adv. Sci.*, 2022, **9**, 2203460.
123 L. Ye, F. Wu, R. Xu, Z. Di, J. Lu, C. Wang, A. Dong, S. Xu, L. Xue, Z. Fan, L. Xu, K. Li, D. Li, A. Kursumovic, R. Zhao, R. Tang, L. Qiu, H. Wang, J. L. MacManus-Driscoll, Q. Jing, W. Li and H. Yang, *Nano Energy*, 2023, **112**, 108460.
124 V. V. Tipparaju, D. Wang, J. Yu, F. Chen, F. Tsow, E. Forzani, N. Tao and X. Xian, *Biosens. Bioelectron.*, 2020, **169**, 112590.
125 J. Suo, Y. Liu, C. Wu, M. Chen, Q. Huang, Y. Liu, K. Yao, Y. Chen, Q. Pan, X. Chang, A. Y. L. Leung, H. Y. Chan, G. Zhang, Z. Yang, W. Daoud, X. Li, V. A. L. Roy, J. Shen, X. Yu, J. Wang and W. J. Li, *Adv. Sci.*, 2022, **9**(31), 2203565.
126 P. V. Adhyapak, A. M. Kasabe, A. D. Bang, J. Ambekar and S. K. Kulkarni, *RSC Adv.*, 2022, **12**, 1157–1164.
127 A. Sinha, A. K. Stavrakis, M. Simić and G. M. Stojanović, *ACS Omega*, 2022, **7**, 44928–44938.
128 Y. Pang, J. Jian, T. Tu, Z. Yang, J. Ling, Y. Li, X. Wang, Y. Qiao, H. Tian, Y. Yang and T.-L. Ren, *Biosens. Bioelectron.*, 2018, **116**, 123–129.
129 J. C. Li, J. Yin, S. Ramakrishna and D. X. Ji, *Biosensors*, 2023, **13**, 205.
130 L. Veeramuthu, R.-J. Weng, W.-H. Chiang, A. Pandiyan, F.-J. Liu, F.-C. Liang, G. R. Kumar, H.-Y. Hsu, Y.-C. Chen, W.-Y. Lin, Y.-C. Tang, W.-R. Lin, R.-J. Chung, T. Zhou and C.-C. Kuo, *Chem. Eng. J.*, 2024, **502**(15), 157752.
131 V. S. Nesic, V. Z. Djordjevic, V. Tomic-Spiric, Z. R. Dudvarski, I. A. Soldatovic and N. A. Arsovic, *J. Laryngol. Otol.*, 2016, **130**, 1064–1071.
132 H. Cheraghi Bidsorkhi, N. Faramarzi, B. Ali, L. R. Ballam, A. G. D'Aloia, A. Tamburrano and M. S. Sarto, *Mater. Des.*, 2023, **230**, 111970.
133 S. Lam, C. MacAulay, J. C. leRiche and B. Palcic, *Cancer*, 2000, **89**, 2468–2473.
134 M. Li, C. L. Zhang, S. C. Deng, L. Li, S. Q. Liu, J. Bai, Y. P. Xu, Y. F. Guan, X. F. Xia, L. Q. Sun, D. P. Carbone and C. P. Hu, *Lung Cancer*, 2021, **162**, 16–22.
135 T. Shaipanich, A. McWilliams and S. Lam, *Respirology*, 2006, **11**, 366–372.
136 A. Ogunpola, F. Saeed, S. Basurra, A. M. Albarrak and S. N. Qasem, *Diagnostics*, 2024, **14**, 144.
137 X. F. Tang, Y. P. Zhu, W. J. Guan, W. J. Zhou and P. F. Wei, *Life Sci.*, 2022, **305**, 120733.
138 Z. Altintas, W. M. Fakanya and I. E. Tothill, *Talanta*, 2014, **128**, 177–186.
139 S. Colagiuri and D. Davies, *Curr. Opin. Endocrinol., Diabetes Obes.*, 2009, **16**, 95–99.
140 P. K. Panakanti, S. Porika and S. K. Yadav, *J. Mech. Continua Math. Sci.*, 2019, **14**, 487–500.
141 P. Zhao, Y. Song, Z. Hu, Z. Zhong, Y. Li, K. Zhou, T. Qin, Y. Yan, H.-H. Hsu, S.-T. Han, V. A. L. Roy, C.-C. Kuo and Y. Zhou, *Nano Energy*, 2024, **130**, 110118.
142 M. R. Li, E. T. H. Chu, C. R. Lee and Ieee, Paris, France, 2024.
143 W. S. Suen, G. Huang, Z. Kang, Y. Gu, J. Fan and D. Shou, *Build. Environ.*, 2021, **205**, 108236.
144 A. Yang, L. Cai, R. Zhang, J. Wang, P.-C. Hsu, H. Wang, G. Zhou, J. Xu and Y. Cui, *Nano Lett.*, 2017, **17**, 3506–3510.
145 Q. Zou, Y. Gai, Y. Cai, X. Gai, S. Xiong, N. Wei, M. Jiang, L. Chen, Y. Liu and J. Gai, *Cellulose*, 2022, **29**, 5711–5724.